Two bump solutions of a homogenized Wilson - Cowan model with periodic microstructure

Elena Malyutina[a], John Wyller[a,*], Arcady Ponosov[a]

[a]*Department of Mathematical Sciences and Technology, P.O. Box 5003, NO-1432 Ås, Norway*

Abstract

We study existence and stability of 2 - bump solutions of the one - population homogenized Wilson - Cowan model, where the heterogeneity is built in the connectivity functions by assuming periodic modulations in both the synaptic footprint and in the spatial scale. The existence analysis reveals that the generic picture consists of two bumps states for each admissible threshold value for the case when the solutions are independent of the local variable and the firing rate function is modeled as a Heaviside function. A framework for analyzing the stability of 2 - bumps is formulated, based on spectral theory for Fredholm integral operators. The stability method deforms to the standard Evans function approach for the translationally invariant case in the limit of no heterogeneity, in a way analogous to the single bump case for the homogenized model. Numerical study of the stability problem reveals that both the broad and narrow bumps are unstable just as in the translationally invariant case when the connectivity function is modeled by means of a wizard hat function. For the damped oscillating connectivity kernel, we give a concrete example of a 2 - bump solution which is stable for all admissible values of the heterogeneity parameter.

Keywords: Rate equations in neuroscience; Periodic; Homogenization

---

*Corresponding author

Email addresses: `elena.malyutina@umb.no` (Elena Malyutina),
`john.wyller@umb.no` (John Wyller), `arkadi.ponossov@umb.no` (Arcady Ponosov)

1. Introduction

Firing rate models have commonly been utilized in the investigation of network properties of the strongly interconnected cortical networks. In neural field models the cortical tissue has in addition been modeled as continuous lines or sheets of neurons. In such models the spatiotemporally varying neural activity is described by one or more scalar fields, one for each neuron type incorporated in the model. These models are formulated in terms of differential, integro - differential equations and integral equations. The most wellknown and simplest model in that respect is the socalled Wilson - Cowan model [1, 2] which in one spatial dimension reads

$$\frac{\partial}{\partial t}u(x,t) = -u(x,t) + \int\limits_{-\infty}^{\infty} \omega(|x' - x|)f(u(x',t))dx' \qquad (1)$$

Here u denotes the average neural activity, ω the coupling strength (referred to as the connectivity function) and f the firing rate function. Notice that the Wilson - Cowan model (1) presupposes that the cortical medium is homogeneous and isotropic.

Since the seminal contributions of Wilson *et al* [1] and Amari [2] several works have been devoted to the study of traveling waves and localized stationary solutions (socalled *bumps*) of this model and its extensions as well as the stability of these coherent structures. In most of these works one assumes that the firing rate function is given by means of the unit step function (Heaviside function), which is mathematically convenient as the traveling waves and the bumps in this case can be given in terms of closed form analytical expressions. The corresponding stability theory is then worked out either by projecting the dynamics of the full system onto a finite dimensional space consisting of the dynamical system in the crossing coordinates between the bumps and the threshold values i.e. pulsewidth coordinates (the *Amari approach*) or by doing a full stability analysis by means of the Evans function approach. See for example Coombes [3] and the references therein.

The simplest type of localized stationary solutions is the *single bump* (or *1 - bump*) of the model (1). For these bumps there is a one - to - one correspondence between the admissible threshold values and the pulsewidth

2

coordinates. The existence and uniqueness of these solutions have been studied in several works, as for example in [2] and Murdock [4] together with their linear stability. Spatially symmetric *2 - bump solutions* of the translationally invariant Wilson - Cowan model are characterized by four intersection points for each threshold value, two positive and two negative. They have been studied in [7, 8, 9]. In Laing *et al* [7] stable and unstable N - bump solutions have been studied numerically, while in Laing *et al* [8] conditions for existence of 2 - bump solutions are established and stability of the bumps state has been assessed by using the Amari technique. Murdock *et al* [9] investigated the existence of symmetric 2 - bump stationary solutions for a class of coupling functions and established their linear stability. All these studies show that the multibumps states in the translationally invariant Wilson - Cowan model are unstable when the connectivity functions are modeled by means of the wizard hat function.

Although the modeling framework given by (1) and its extensions qualitatively are expected to capture the essential features of the brain activity on the macroscale level, they do not account for the heterogeneity in the cortical structure. Thus they represent a simplification of the actual situation. Therefore it is a pressing need to develop mathematical tools for the study of waves and bumps in heterogeneous media that can be used in brain modeling. One common tool which could be useful in the study of such problems is homogenization techniques [10, 11]. This multiscale approach leads to the study of effective constant coefficient equations termed homogenized equations when dealing with partial differential equations. In the case of periodic microstructure the homogenization involves averaging over some well identified micro - scale. Bressloff [12] was the first to extend this technique to neural field models and to show how to describe fronts that travel through a neural model with a periodically modulated microstructure. The experimental findings suggest that there is a periodic microstructure in the primary visual cortex. Coupling between periodic micro level structure of the cortex and nonlocal mean field description has been addressed in some other papers as well [13, 14, 15, 16, 17]. It turns out that the detailed microstructure has an impact on pattern forming mechanisms as well as existence and stability of traveling fronts and pulses. A common feature observed in [13, 14, 15, 16, 17] is the propagation failure when the wave speed is too slow or the degree of heterogeneity too large.

Conventional homogenization procedures consist of techniques which are wellknown in the applied mathematics community such as perturbation expansions (see for example Persson *et al* [18] and the references therein). Modern homogenization theory based on multi - scale convergence techniques represents an alternative approach to this problem. It provides efficient and rigorous methods for studying the coupling between the microstructure and macroscopic levels. This approach to homogenization theory was originally presented by Nguetseng [19]. A careful treatment of the theoretical foundation of the method can be found in Lukkasen *et al* [20]. The multiscale approach of Nguetseng has successfully been applied to homogenization of partial differential equations (see for example Lukkassen *et al.* [20] and the references therein). Apart from the works [21, 22, 23], it seems not to be very wellknown in the mathematical neuroscience community.

In Svanstedt *et al* [21, 22] it is proved that the one - parameter family of one population Wilson-Cowan models with periodic microstructure

$$\frac{\partial}{\partial t}u_\varepsilon(x,t) = -u_\varepsilon(x,t) + \int_\Omega \omega(x'-x, \frac{x'-x}{\varepsilon})f(u_\varepsilon(x',t))dx', \quad x \in \Omega, \quad t > 0$$

(2)

two scale converges to

$$\frac{\partial}{\partial t}u(x,y,t) = -u(x,y,t) + \int_\Omega dx' \int_Y dy'\omega(x'-x,y'-y)f(u(x',y',t)) \quad (3)$$

for $x \in \Omega, y \in Y, t > 0$ when $\varepsilon \to 0$. Here Ω is a subset of $\mathbb{R}^k$ and $Y = [0,1]^k$. The connectivity kernel ω is periodic in the second variable $y = x/\varepsilon$ with Y as a period cell. In Coombes *et al* [23] the model (3) was used in a study of traveling fronts in a medium with periodic structure, while in Svanstedt *et al* [22] existence and stability of y - independent single bump solutions of the homogenized Wilson - Cowan model (3) are studied when the firing rate function is given by means of the Heaviside function. In the latter paper the existence and uniqueness issue is studied by means of the pinning function technique using the heterogeneity parameter as a control parameter. In Svanstedt *et al* [22] the stability problem is resolved by means of the spectral properties of a Hilbert - Schmidt integral operator in the microvariable y. The spectrum of this operator is computed by means of a Fourier decomposition method in a way analogous to single bump solutions

4

of the homogeneous translational invariant Wilson - Cowan model in two spatial dimensions [24] and the spectral stability of vortex solutions to the Gross - Pitaevski equation in a two dimensional spatial configuration [25]. This method can be viewed as yielding an Evans function for each Fourier mode in a way analogous to the homogeneous translationally invariant case (see for example Coombes [3] and the references therein). It turns out that the stability properties can be deduced from the monotonicity properties of the pinning function alone: Stable (unstable) bumps correspond to excitation widths for which the pinning function is strictly increasing (decreasing). In [22] this theory is illustrated when the connectivity function is given as an exponentially decaying function, a wizard hat function and a damped oscillating function, where the functions are periodically modulated in the synaptic footprint as well in the spatial scale. In the wizard hat function case bumps cannot exist for strong heterogeneity. Just as in the translationally invariant Wilson - Cowan case with a wizard hat connectivity function there is regime of threshold values producing two types of single bumps for each threshold value, one *narrow* bump and one *broad* bump. The narrow (broad) bump is always unstable, which can be deduced from the fact that the pinning function is strictly increasing (decreasing) for the excitation width of this bump.

This serves as a background for the present work. We study the existence, uniqueness and stability of spatially symmetric 2 - bump solutions within the framework of the homogenized model (3). The existence and uniqueness issue is dealt with in a way analogous to Blomquist *et al* [26] and Yousaf *et al* [27] for single bump solutions in a two population model of excitatory and inhibitory neurons: As the number of positive intersection points (pulsewidths) between the spatially symmetric 2 - bump solutions and the threshold values are two, we conveniently study the existence of 2 - bump solutions by viewing the pinning equation problem as a one - parameter family of mapping problems from the set of pulse widths to the threshold value plane with the heterogeneity parameter as a parameter. The uniqueness problem is a local problem which is studied by considering the solution of the pinning equations as points for transversal intersection of level curves. We find that 2 - bump solutions exist for small and moderate values of the threshold value for firing while we have non - existence of bumps when threshold value exceeds a certain critical value. This critical value depends on the heterogeneity parameter. We also show that the generic picture consists of one broad and

5

one narrow 2 - bump solution in the regime of small and moderate values of the threshold value for firing. Notice that our geometrical approach is different from the method used in Murdock *et al* [9] to establish necessary conditions for the existence of 2 - bumps. In the latter paper the number of 2 - bump solutions as a function of the threshold value is not studied. The stability problem boils down to a study of the spectrum for a Fredholm integral operator. We compute the spectrum of this operator by using the Fourier decomposition method in a way analogous to Svanstedt *et al* [22] for the single bumps case. We show that our stability method deforms to the Evans function technique of Murdock *et al* [9] when switching off the effect of heterogeneity. A notable feature is that the actual integral operator for the stability problem is not a Hilbert - Schmidt integral operator as in the single bumps case, but a nonsymmetric Fredholm integral operator. The reason for this is that the slopes of the bumps evaluated at the pulse width coordinates are different. Finally, we give concrete examples on the application of the present stability approach in the case when the connectivity kernel is given by means of a modulated wizard hat function and a damped oscillating function. For the wizard hat function numerical computations indicate that both the narrow and the broad 2 - bumps remain unstable when switching on the heterogeneity, while in the example with the periodically modulated damped oscillating connectivity function the 2 - bumps remain stable when switching on the heterogeneity.

The present work is organized in the following way: Section 2 is devoted to the existence and uniqueness of 2 - bump solutions. In Section 3.1 we formulate the general framework for analyzing the stability of 2 - bump solutions. In Section 3.2 we give concrete examples on the application of this theory to cases where the connectivity function is given as a modulated wizard hat function and a damped oscillating function. Section 4 contains conclusions and an outlook.

2. Existence and uniqueness of 2 - bump solutions

In this section we study the existence and uniqueness of 2 - bump solutions of the homogenized Wilson - Cowan model (3) when we assume $\Omega = \mathbb{R}$ $(k = 1)$. It is assumed that these solutions are independent of the local variable y, i.e. $u(x, y, t) = U(x)$. We proceed in a way analogous to Svanstedt *et al* [22].

6

We find that if stationary solutions U exist, they must satisfy the fixed point problem

$$U(x) = \int\limits_{-\infty}^{\infty} f(U(x'))\langle\omega\rangle(x' - x)dx' \tag{4}$$

where $\langle\omega\rangle$ denotes the average of the connectivity function ω over the unit cell i.e.

$$\langle\omega\rangle(x) = \int\limits_{0}^{1} \omega(x, y)dy \tag{5}$$

The next step consists of approximating the firing rate function f by means of the Heaviside step function H: $f(u) = H(u - \theta)$. Here θ is the threshold value for firing of the neuronal population. We assume that $0 < \theta \leq 1$. The construction of spatially symmetric 2 - bump solutions proceeds in the following way: We assume that the equation $U(x) = \theta$ has four solutions $\pm a$ and $\pm b$, such that $0 < a < b$. Moreover, U obeys the conditions

$$U(x) = U(-x), \quad U(\pm\infty) = 0$$

$$U(x) > \theta, \quad a < |x| < b \tag{6}$$

$$U(x) < \theta, \quad |x| < a, |x| > b$$

In a way analogous to the translationally invariant case, we express the 2 - bump solutions in terms of the anti-derivative W of $\langle\omega\rangle$ i.e.

$$W(x) \equiv \int\limits_{0}^{x} \langle\omega\rangle(z)dz \tag{7}$$

We get

$$U(x) = W(x + b) - W(x + a) + W(x - a) - W(x - b) \tag{8}$$

Notice that $U(x) \equiv 0$ when $a = b$. Now, by making use of the stationarity assumptions (6) and (8), we end up with the system of equations for the pulse width coordinates a and b given as

$$F(a, b) = \theta$$

$$\tag{9}$$

$$G(a, b) = 0$$

7

where F and G are defined by

$$F(a,b) \equiv W(b-a) - W(b+a) + W(2b)$$

$$G(a,b) \equiv W(2b) + W(2a) - 2W(b+a)$$

(10)

The system (9) with F and G given by (10) is referred to as *the set of pinning equations.*

In the present work we assume that the connectivity function ω is expressed in terms of a continuous and absolute integrable scaling function φ i.e.

$$\omega(x,y) = \frac{1}{\sigma(y)} \varphi\left[\frac{x}{\sigma(y)}\right]$$

(11)

The synaptic footprint function σ is assumed to be periodic with period 1, even, continuous and strictly positive. This means that the connectivity function ω is periodically modulated in the local scale y. Just as in Svanstedt *et al* [22], we assume that

$$\sigma(y) = 1 + \gamma \cos(2\pi y), \quad 0 \leq \gamma < 1$$

(12)

The parameter γ which measures the degree of heterogeneity, is referred to as the *heterogeneity parameter*. Notice that the case $\gamma = 0$ corresponds to the 2 - bump solution in the translationally invariant case. In the present work we study existence and stability of 2 - bumps in two concrete cases: In the first case the scaling function $\varphi(\xi)$ is given by the *wizard hat function*

$$\varphi[\xi] = e^{-|\xi|}(1 - \alpha|\xi|)$$

(13)

while in the second case it assumes the form of the damped oscillating function

$$\varphi[\xi] = Ke^{-\beta|\xi|}(\cos(\alpha|\xi|) + \beta \sin(\alpha|\xi|)), \quad K, \alpha, \beta > 0$$

(14)

The anti - derivative W defined by (7) now becomes a 1 - parameter family of functions parameterized by γ. The particular form (11) for the connectivity function leads to the expression

$$W(x;\gamma) = \int_0^1 \int_0^{\frac{x}{\sigma(y)}} \varphi[\xi]d\xi dy$$

(15)

8

The functions F and G defined by (10) hence depend on γ, i.e.

$$F(a, b; \gamma) \equiv W(b - a; \gamma) - W(b + a; \gamma) + W(2b; \gamma)$$

$$G(a, b; \gamma) \equiv W(2b; \gamma) + W(2a; \gamma) - 2W(b + a; \gamma)$$

(16)

with the corresponding set of pinning equations

$$F(a, b; \gamma) = \theta$$

$$G(a, b; \gamma) = 0$$

(17)

Now, let us address the issue of existence and uniqueness of 2 - bump solutions. The question about existence of bumps solutions simplifies to existence of solutions to the system (16) - (17). We conveniently study this problem by using a mapping technique which is analogous to the one used in [26, 27] for the existence of single bumps solutions of two population model.

We proceed as follows: Let us introduce the subsets Σ and I of $\mathbb{R}^2$ defined

$$\Sigma = \{(a, b) \in \mathbb{R}^2 | 0 < a \leq b\}$$

$$I = \{(\theta, \widetilde{\theta}) \in \mathbb{R}^2 | 0 < \theta \leq 1, \widetilde{\theta} = 0\}$$

Moreover, introduce the vectors $\underline{a}$ and $\underline{\theta}$ defined by

$$\underline{a} = \begin{bmatrix} a \\ b \end{bmatrix}, \qquad \underline{\theta} = \begin{bmatrix} \theta \\ \widetilde{\theta} \end{bmatrix}$$

where $\theta \geq 0$, $\widetilde{\theta} \in \mathbb{R}$ and $\underline{a} \in \Sigma$. Then introduce the 1-parameter family of vectorfields $\underline{F}_\gamma : \Sigma \to \mathbb{R}^2$ parameterized by γ defined by

$$\underline{\theta} = \underline{F}_\gamma(\underline{a}) = \begin{bmatrix} F(a, b; \gamma) \\ G(a, b; \gamma) \end{bmatrix}$$

(18)

where the component functions F and G are defined by (16).

We get the following result:

Theorem 1. $\underline{F}_\gamma(\Sigma)$ *is a bounded subset of* $\mathbb{R}^2$.

9

PROOF. The triangle inequality yields

$$|F(a,b;\gamma)| \le |W(b-a;\gamma)| + |W(b+a;\gamma)| + |W(2b;\gamma)|$$

$$|G(a,b;\gamma)| \le |W(2b;\gamma)| + 2|W(b+a;\gamma)| + |W(2a;\gamma)|$$

For convenience we have introduced

$$\begin{aligned}
\beta_1(a,b) &= b - a \\
\beta_2(a,b) &= b + a \\
\beta_3(a,b) &= 2b \\
\beta_4(a,b) &= 2a
\end{aligned}$$

Then we get

$$|W(\beta_i(a,b),\gamma)| = \left| \int_0^1 \int_0^{\frac{\beta_i(a,b)}{\sigma(y)}} \varphi(\xi)d\xi dy \right| \le \int_0^1 \int_0^{\frac{\beta_i(a,b)}{\sigma(y)}} |\varphi(\xi)|d\xi dy$$

Since φ by assumption is absolute integrable, we get

$$|W(\beta_i(a,b),\gamma)| < \infty$$

from which it follows that $\underline{F}_\gamma(\Sigma)$ is a bounded subset of $\mathbb{R}^2$. $\qquad\square$

In Fig.1 we show the image of the region Σ under the vector field $\underline{F}_\gamma$ when the connectivity function is given by the wizard hat function (11) - (13) for two different values of the heterogeneity parameter γ i.e $\gamma = 0$ and $\gamma = 0.7$. First of all, these plots show that the subset $\underline{F}_\gamma(\Sigma)$ is bounded, in accordance with Theorem 1. Secondly, we observe that the intersection $\underline{F}_\gamma(\Sigma) \cap I$ is non - empty, i.e. there is a θ_{cr} which depends on γ such that

$$\underline{F}_\gamma(\Sigma) \cap I = \{(\theta, \widetilde{\theta}) | 0 < \theta \le \theta_{cr} < 1, \widetilde{\theta} = 0\} \tag{19}$$

In this case we conclude that for $\theta \in (0, \theta_{cr}]$ the system (16) - (17) has at least one solution, from which we conclude that there exists at least one 2 - bump solution in this case. The subinterval $(0, \theta_{cr}]$ is referred to as *the interval of admissible threshold values*. The critical threshold value θ_{cr}, which is a

10

function of the heterogeneity parameter γ, is determined by means of the non - transversality condition

$$\det \left[\frac{\partial \underline{F}_\gamma}{\partial \underline{a}}\right](\underline{a}) = 0$$

(20)

$$F(a, b; \gamma) = \theta_{cr}(\gamma), \quad G(a, b; \gamma) = 0$$

For $\theta_{cr}(\gamma) < \theta < 1$, the pinning equations (16) - (17) have no solutions, corresponding to non - existence of 2 - bumps. Fig. 2 shows the existence of 2 - bumps as a function of the heterogeneity parameter γ and the threshold value θ. The computation underlying the plot of the separatrix curve $\theta = \theta_{cr}(\gamma)$ separating regions producing 2 - bump solutions from the non - existence regime is based on the condition (20).

Next, we study the number of solutions of the pinning equation system (16) - (17) i.e. the number of solutions to the fixed point problem (4) for a given admissible threshold value $\theta \in (0, \theta_{cr}(\gamma)]$. We denote the solution of this system as $\underline{a} = (a, b)$. Since the connectivity function ω is continuous in (x, y), the vector field $\underline{F}_\gamma$ defined by means of the component functions in (16) is continuously differentiable on Σ. Just as in Blomquist *et al* [26] the generic picture consists of two 2 - bumps for small and moderate values of the threshold value, i.e. for each threshold value in the open subinterval $(0, \theta_{cr}(\gamma))$. To show this we proceed as follows: We view the system of equations (17) as level curves of the component functions (16) with level curve constants θ and 0. The existence of 2 - bumps is then translated into a study of intersection of these level curves. By adjusting the threshold value θ to be just below $\theta_{cr}(\gamma)$, we get two intersection points locally which correspond to two 2 - bumps, i.e. one *narrow* and one *broad* 2 - bump. Fig. 3 demonstrates this behavior. The inverse function theorem now shows that the Jacobian of $\underline{F}_\gamma$ at the point $\underline{a}$ is non-singular, i.e.

$$\det \left[\frac{\partial \underline{F}_\gamma}{\partial \underline{a}}\right](\underline{a}) \neq 0 \qquad (21)$$

for each of the intersection points, which means by the inverse function theorem guarantees local uniqueness of the solution of the pinning equation system (16) - (17) for a given value of γ. Fig.4 shows examples of transversal

11

intersection of the level curves (16) - (17) for different values of the heterogeneity parameter γ when θ belongs to the set of admissible threshold values. The corresponding narrow and broad 2 - bump solutions are displayed in Fig. 5. Fig. 6 shows examples of non - transversal intersection of the level curves, corresponding to coalescence of a broad - and narrow 2 - bump at the critical threshold value $\theta_{cr}(\gamma)$ as demonstrated in Fig. 7. For the sake of completeness, we also show examples of non - crossing of the level curves (16) - (17), corresponding to non - existence of 2 - bump solutions (Fig. 8).
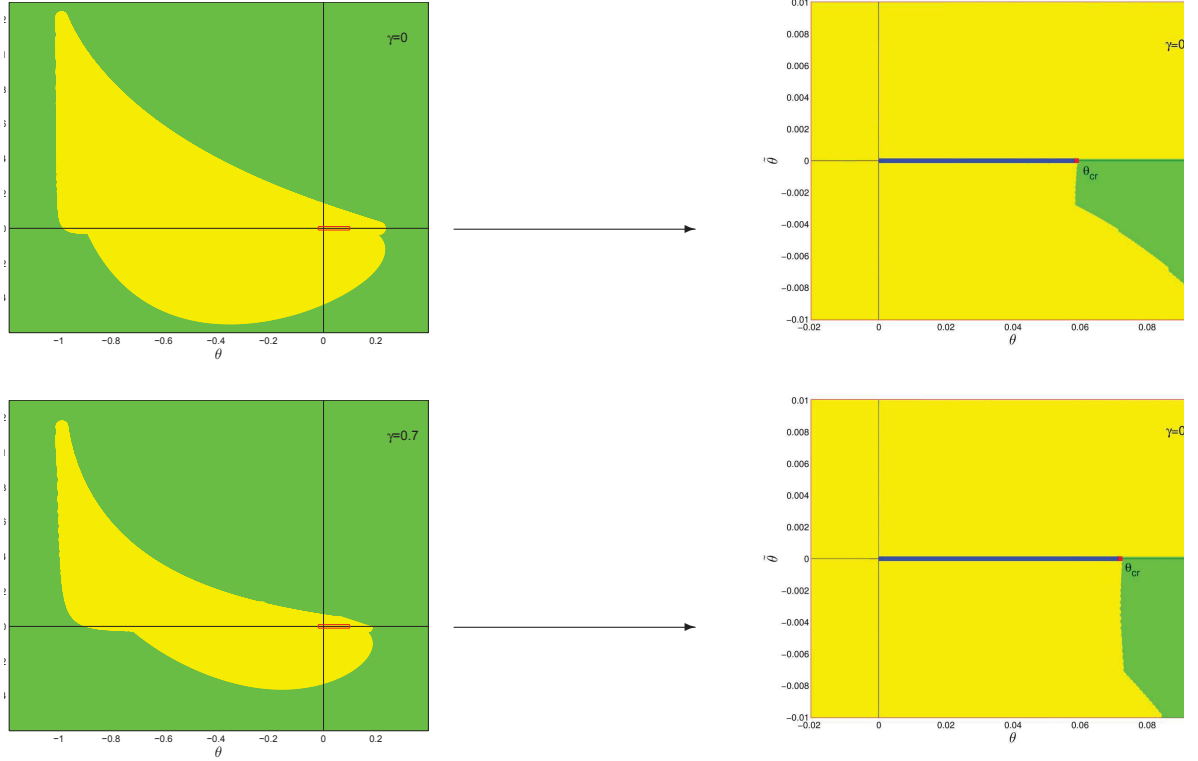
Figure 1: The image of $\Sigma = \{(a,b)|b \geqslant a > 0\}$ in $\mathbb{R}^2$, $0 < \theta \leqslant 1$ under the mapping $\underline{F}_\gamma$ is the yellow region, while the complement set $\mathbb{R}^2 \setminus \underline{F}_\gamma(\Sigma)$ is green. The intersection $\underline{F}_\gamma(\Sigma) \cap I$ is marked with blue, while the critical threshold value θ_{cr} for existence of 2 - bumps is marked with a red point. Input data: The scaling function φ is given by (13), $\alpha = 2$, $\gamma = 0$, $\gamma = 0.7$. The right column of figures gives magnified view of rectangular regions marked in the left column of figures.

13
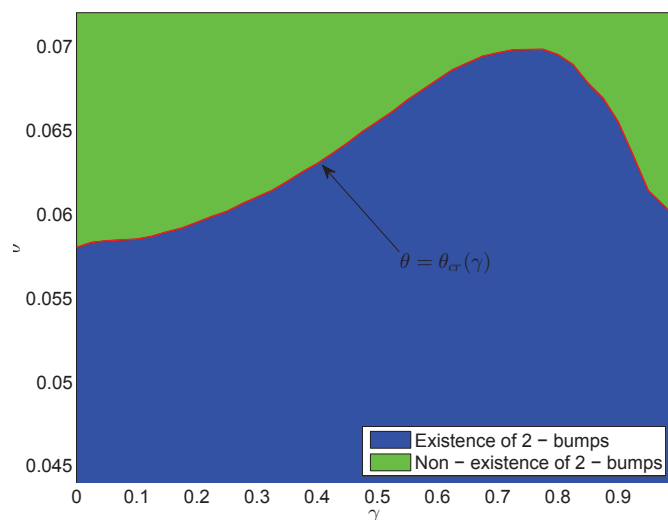
Figure 2: Existence and non - existence of 2 - bump solutions as a function of the heterogeneity parameter γ and the threshold value θ. Blue region corresponds to existence of bumps, green region to non - existence and red curve to the separatrix curve $\theta = \theta_{cr}(\gamma)$, in accordance with Fig. 1. The scaling function φ is given by the wizard hat function (13) with $\alpha = 2$. The curve $\theta = \theta_{cr}(\gamma)$ is determined by means of (20).
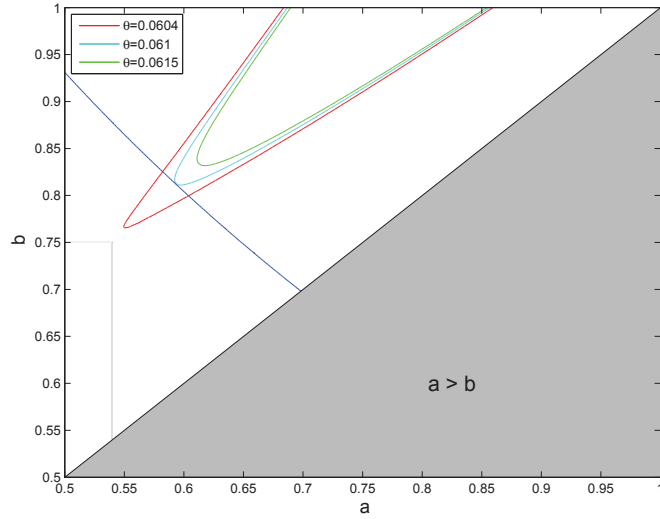
Figure 3: Generation of 2 - bumps for a fixed value of the heterogeneity parameter γ in the pulse width coordinate plane. The threshold value θ is in the vicinity of θ_{cr} in the pulse width coordinate plane The scaling function φ is given by the wizard hat function (13) with $\alpha = 2$. The grey shaded region corresponds to the forbidden sector $a > b$ in the first quadrant of the pulse width coordinate plane. Blue curve: $G(a, b; \gamma) = 0$. Input data: $\theta = 0.0615$ (green curve, no intersection of level curves (16) - (17), no 2 - bumps), $\theta = \theta_{cr}(0.3) = 0.061$ (cyan curve, non - transversal intersection of level curves (16) - (17), one 2 - bump), and $\theta = 0.0615$ (red curve, transversal intersection of level curves (16) - (17), two 2 - bumps) and $\gamma = 0.3$.

15
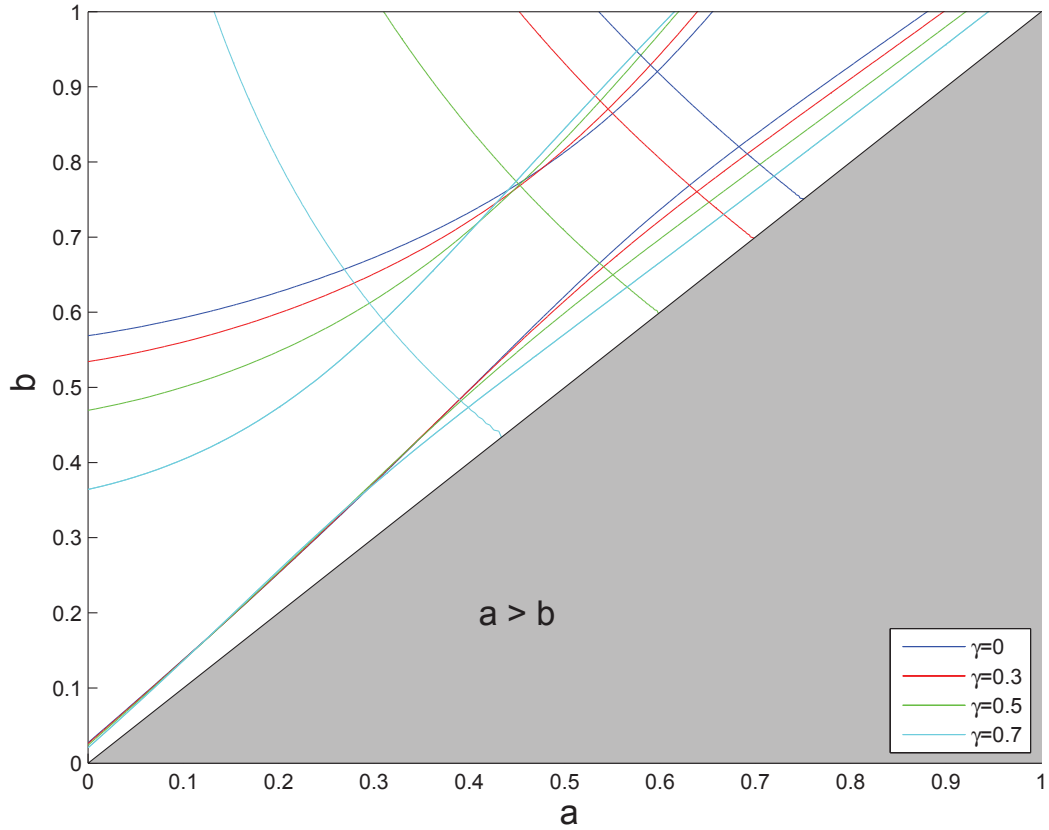
Figure 4: Transversal intersection of the level curves (16) - (17) for different values of the heterogeneity parameter γ and a fixed threshold value θ ($\theta = 0.05$). The scaling function φ is given by the wizard hat function (13) with $\alpha = 2$. The grey shaded region corresponds to the forbidden sector $a > b$ in the first quadrant of the pulse width coordinate plane.

(a)

(b)
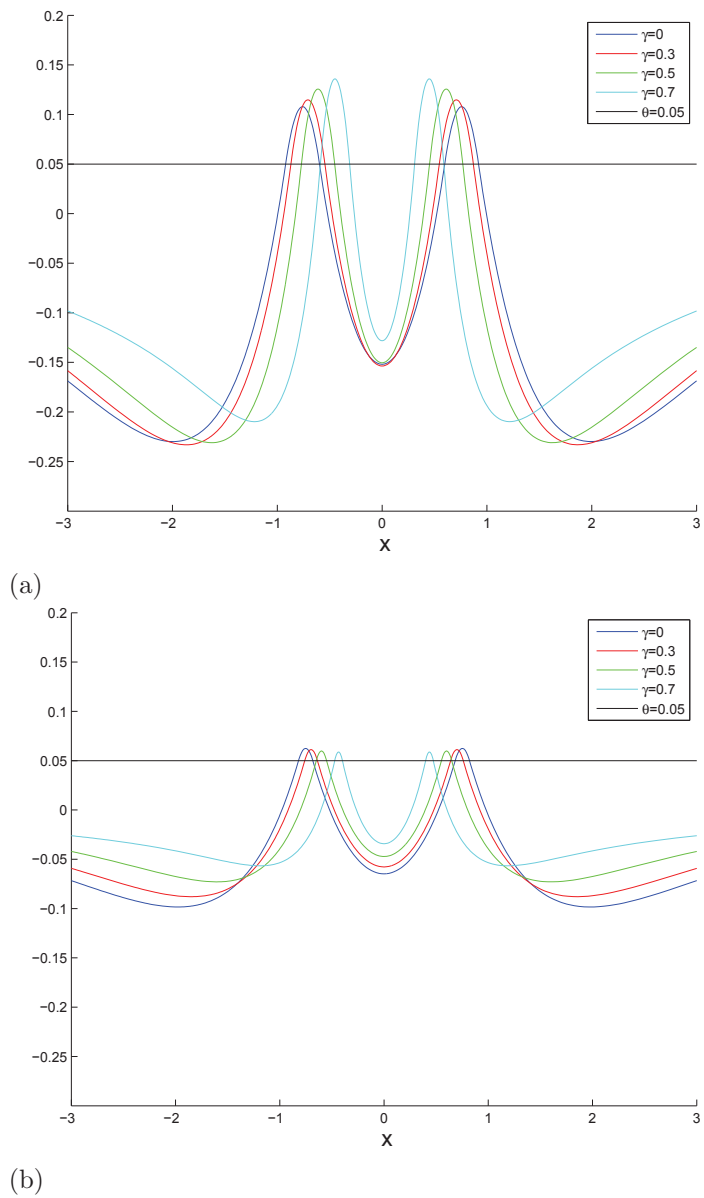
Figure 5: Broad (a) and narrow (b) 2 - bump solutions corresponding to the transversal intersections of the level curves (16) - (17) displayed in Fig. 4. The scaling function φ is given by the wizard hat function (13) with $\alpha = 2$.

17
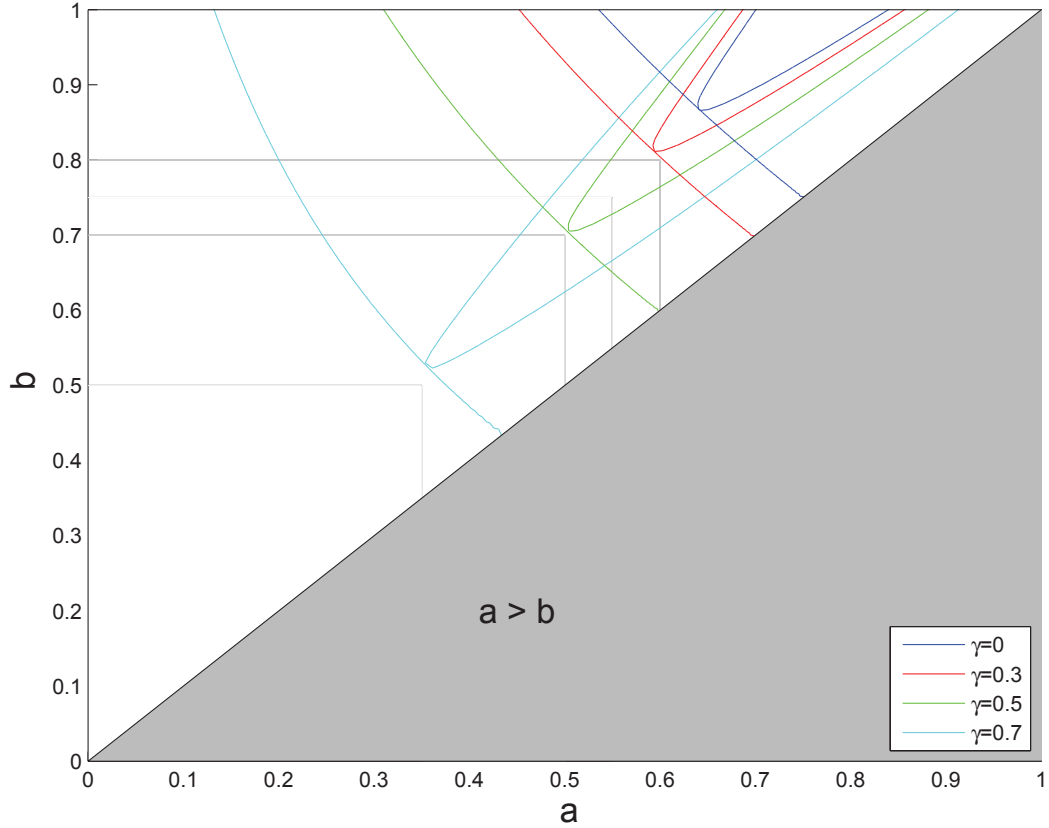
Figure 6: Non - transversal intersection of the level curves (16) - (17) for different values of the heterogeneity parameter γ and critical threshold values $\theta = \theta_{cr}(\gamma)$. The scaling function φ is given by the wizard hat function (13) with $\alpha = 2$. The grey shaded region corresponds to the forbidden sector $a > b$ in the first quadrant of the pulse width coordinate plane.
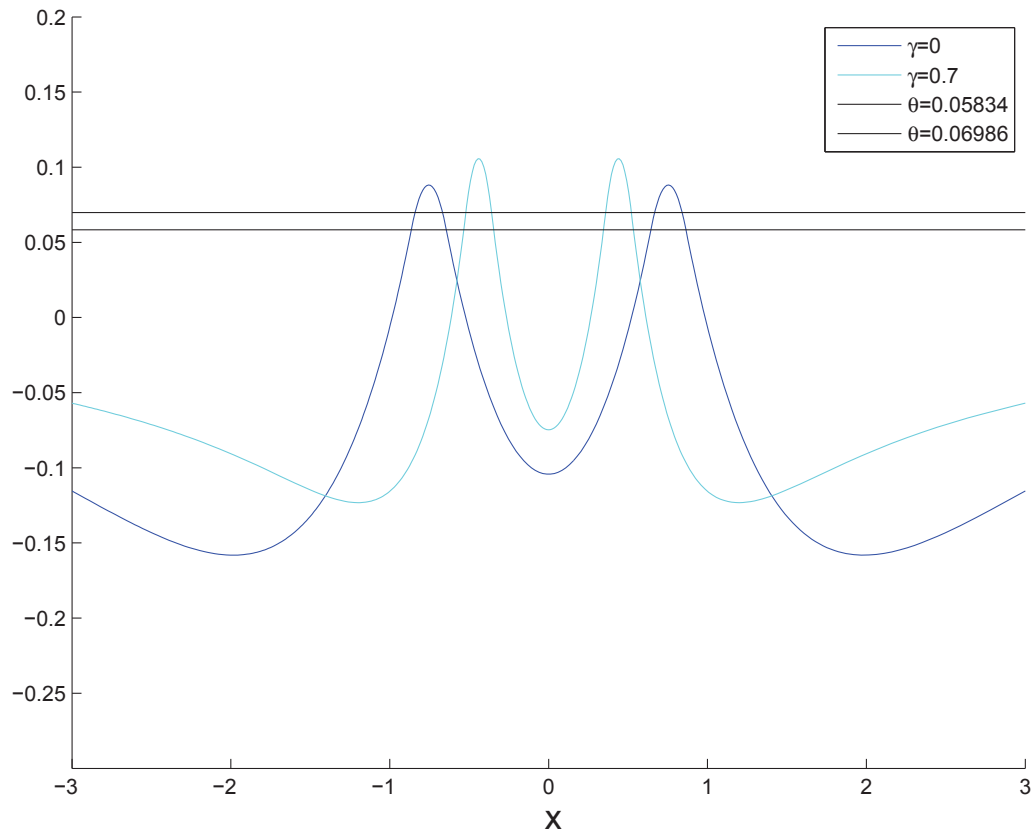
Figure 7: 2 - bump solutions in the case of non - transversal intersections of the level curves (16) - (17) displayed in Fig. 6 for $\gamma = 0$ (blue curves) and $\gamma = 0.7$ (cyan curves). The scaling function φ is given by the wizard hat function (13) with $\alpha = 2$.
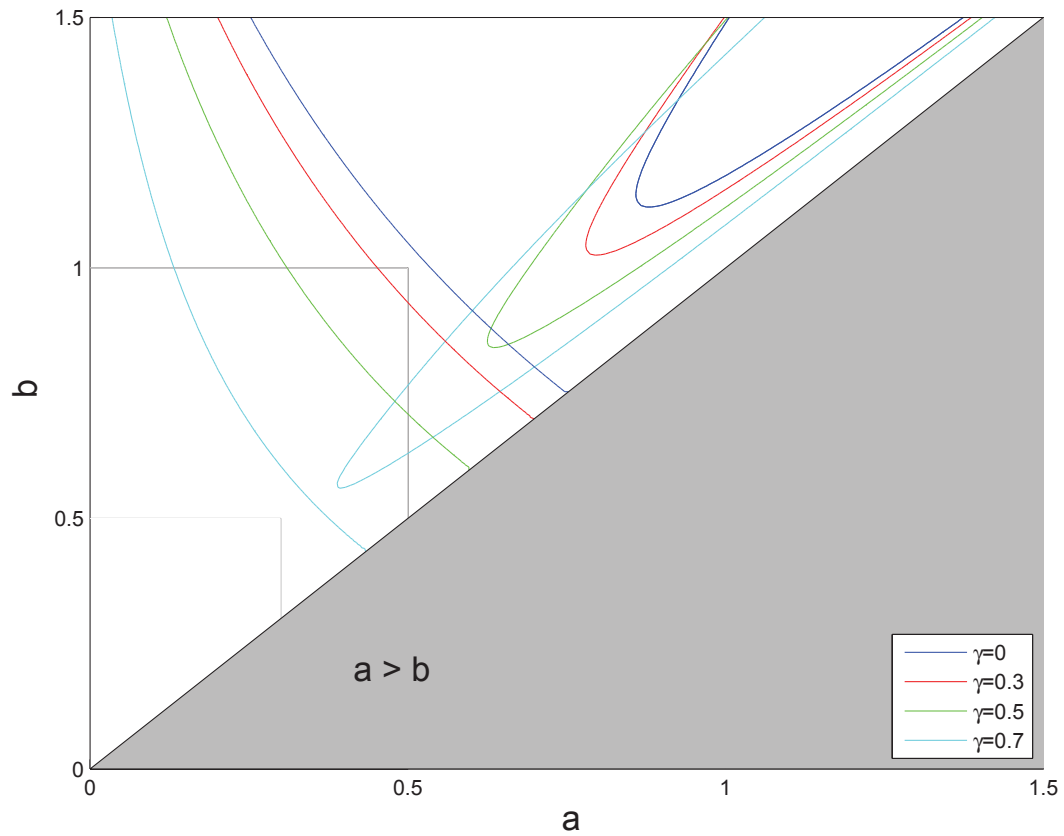
Figure 8: Non - existence of 2 - bump solutions corresponding to non - intersecting level curves (16) - (17) for different values of the heterogeneity parameter γ and a fixed threshold value θ ($\theta = 0.071$). The scaling function φ is given by the wizard hat function (13) with $\alpha = 2$. The grey shaded region corresponds to the forbidden sector $a > b$ in the first quadrant of the pulse width coordinate plane.

3. Stability analysis

3.1. General framework

In this section we develop a general framework for studying the stability of 2 - bump solutions within the framework of the homogenized Wilson-Cowan model. We proceed in a way analogous to Svanstedt *et al* [22] for the single bumps. We impose the perturbations

$$u(x, y, t) = U(x) + \Phi(x, y, t), \quad |\Phi(x, y, t)| \ll |U(x)|$$

on the bump state and linearize the nonlocal evolution equation for the perturbation Φ. Then, by assuming $\Phi(x, y, t) = \Psi(x, y)e^{\lambda t}$ we end up with the linear nonlocal amplitude equation for Ψ i.e.

$$(\lambda + 1)\Psi(x, y) = \int_{-\infty}^{\infty} dx' \int_0^1 dy' \omega(x' - x, y' - y)H'(U(x') - \theta)\Psi(x', y') \quad (22)$$

The integral term on the right hand side can be computed by taking into account the definition of the 2 - bump solution. We readily obtain

$$(\lambda + 1)\Psi(x, y) = \int_0^1 \left[\frac{\omega(b+x, y'-y)}{|U'(b)|}\Psi(-b, y') + \frac{\omega(a+x, y'-y)}{|U'(a)|}\Psi(-a, y') + \right. \tag{23}$$
$$\left. + \frac{\omega(a-x, y'-y)}{|U'(a)|}\Psi(a, y') + \frac{\omega(b-x, y'-y)}{|U'(b)|}\Psi(b, y')dy' \right]$$

By inserting $x = -b$, $x = -a$, $x = a$, $x = b$ into (22) we otain the four linear equations

$$(\lambda + 1)\Psi(-b, y) =$$
$$\frac{1}{|U'(b)|} \int_0^1 [\omega(0, y'-y)\Psi(-b, y') + \omega(2b, y'-y)\Psi(b, y')]dy' + \tag{24a}$$
$$+ \frac{1}{|U'(a)|} \int_0^1 [\omega(b-a, y'-y)\Psi(-a, y') + \omega(b+a, y'-y)\Psi(a, y')]dy'$$

$$(\lambda + 1)\Psi(-a, y) =$$
$$\frac{1}{|U'(b)|} \int_0^1 [\omega(b-a, y'-y)\Psi(-b, y') + \omega(b+a, y'-y)\Psi(b, y')]dy' + \tag{24b}$$
$$+ \frac{1}{|U'(a)|} \int_0^1 [\omega(0, y'-y)\Psi(-a, y') + \omega(2a, y'-y)\Psi(a, y')]dy'$$

21

$$(\lambda + 1)\Psi(a, y) =$$

$$\frac{1}{|U'(b)|} \int_0^1 [\omega(b + a, y' - y)\Psi(-b, y') + \omega(b - a, y' - y)\Psi(b, y')]dy' +$$

$$+ \frac{1}{|U'(a)|} \int_0^1 [\omega(2a, y' - y)\Psi(-a, y') + \omega(0, y' - y)\Psi(a, y')]dy' \qquad (24c)$$

$$(\lambda + 1)\Psi(b, y) =$$

$$\frac{1}{|U'(b)|} \int_0^1 [\omega(2b, y' - y)\Psi(-b, y') + \omega(0, y' - y)\Psi(b, y')]dy' +$$

$$+ \frac{1}{|U'(a)|} \int_0^1 [\omega(b + a, y' - y)\Psi(-a, y') + \omega(b - a, y' - y)\Psi(a, y')]dy' \qquad (24d)$$

Let

$$\underline{\Psi}(y) = \begin{bmatrix} \Psi(-b, y) \\ \Psi(-a, y) \\ \Psi(a, y) \\ \Psi(b, y) \end{bmatrix}$$

Then the system (24) can be written as the eigenvalue problem

$$\mathbb{H}\underline{\Psi} = \mu\underline{\Psi} \qquad (25)$$

for the integral operator $\mathbb{H}$ defined as

$$[\mathbb{H}\underline{\Phi}](y) = \int_0^1 \mathbb{W}(y - y')\underline{\Phi}(y')dy' \qquad (26)$$

with

$$\mathbb{W}(y) = \begin{bmatrix} c_1\omega(0, y) & c_2\omega(b - a, y) & c_2\omega(b + a, y) & c_1\omega(2b, y) \\ c_1\omega(b - a, y) & c_2\omega(0, y) & c_2\omega(2a, y) & c_1\omega(b + a, y) \\ c_1\omega(b + a, y) & c_2\omega(2a, y) & c_2\omega(0, y) & c_1\omega(b - a, y) \\ c_1\omega(2b, y) & c_2\omega(b + a, y) & c_2\omega(b - a, y) & c_1\omega(0, y) \end{bmatrix}$$

and

$$\underline{\Phi}(y) = \begin{bmatrix} \Phi_1(y) \\ \Phi_2(y) \\ \Phi_3(y) \\ \Phi_4(y) \end{bmatrix}$$

Here the relationship between the eigenvalue μ and the growth/decay rate λ is given as

$$\mu = (\lambda + 1)|U'(a)||U'(b)| \qquad (27)$$

where the slope parameters $c_1 \equiv |U'(a)|$ and $c_2 \equiv |U'(b)|$ are given as

$$c_1 = \langle\omega\rangle(0) - \langle\omega\rangle(2a) + \langle\omega\rangle(b+a) - \langle\omega\rangle(b-a)$$

$$c_2 = \langle\omega\rangle(0) - \langle\omega\rangle(2b) + \langle\omega\rangle(b+a) - \langle\omega\rangle(b-a) \qquad (28)$$

The key issue now consists of determining the spectrum of the operator $\mathbb{H}$. We first notice that this operator is a compact linear operator (Fredholm integral operator). A wellknown result in the theory of such operators states that all $\mu \neq 0$ are either eigenvalues of the operator or do not belong to the spectrum at all. (See for example Porter *et al* [28] and Kolgomorov *et al* [29]). The only possible element in the essential spectrum is 0. This point is the accumulation point of the sequence of eigenvalues as $n \to \infty$. Moreover, it will not influence the stability assessment.

We next compute the eigenvalues of the operator $\mathbb{H}$ by using the Fourier decomposition method in a way analogous to Owen *et al* [24] for single bumps in two spatial dimensions, Kollár *et al* [25] for the spectral stability of vortex solutions to the Gross - Pitaevski equation in a two dimensional spatial configuration and Svanstedt *et al* [22] for the stability of a single bumps in the homogenized Wilson - Cowan model (3). The following theorem summarizes the result of this computation:

Theorem 2. *Let $\widetilde{\mathbb{M}}_n$ and $\widetilde{\mathbb{L}}_n$, $n = 0, 1, 2, 3, ...$ be the 2×2 matrices*

$$\widetilde{\mathbb{M}}_n = \begin{bmatrix} c_1\beta_{n,M} & c_2\delta_{n,M} \\ c_1\delta_{n,M} & c_2\alpha_{n,M} \end{bmatrix} \qquad (29)$$

and

$$\widetilde{\mathbb{L}}_n = \begin{bmatrix} c_2\alpha_{n,L} & c_1\delta_{n,L} \\ c_2\delta_{n,L} & c_1\beta_{n,L} \end{bmatrix} \qquad (30)$$

23

where $\alpha_{n,j}$, $\beta_{n,j}$ and $\delta_{n,j}$, $j = M, L$, $n = 0, 1, 2, ...$ are given as

$$\alpha_{n,L} = \widetilde{\omega}_n(0) - \widetilde{\omega}_n(2a), \quad \alpha_{n,M} = \widetilde{\omega}_n(0) + \widetilde{\omega}_n(2a)$$

$$\beta_{n,L} = \widetilde{\omega}_n(0) - \widetilde{\omega}_n(2b), \quad \beta_{n,M} = \widetilde{\omega}_n(0) + \widetilde{\omega}_n(2b) \tag{31}$$

$$\delta_{n,L} = \widetilde{\omega}_n(b-a) - \widetilde{\omega}_n(b+a), \quad \delta_{n,M} = \widetilde{\omega}_n(b-a) + \widetilde{\omega}_n(b+a)$$

Here $\widetilde{\omega}_n$, $n = 0, 1, 2, ...$ denotes the Fourier coefficients

$$\widetilde{\omega}_n(x) = \int\limits_0^1 \omega(x, y) \exp[-i2\pi ny] dy \tag{32}$$

of the connectivity kernel $\omega(x, y)$ with respect to the local variable y.

Then the eigenvalues of the integral operator $\mathbb{H}$ defined by (26) are given in terms of four sequences $\{\mu_{n,j}^{\pm}\}$, $n = 0, 1, 2, ...$, $j = M, L$ where

$$\mu_{n,j}^{\pm} = \frac{1}{2}[c_1\beta_{n,j} + c_2\alpha_{n,j} \pm \sqrt{D_{n,j}}] \tag{33}$$

where the positive discriminants $D_{n,j}$ are given as

$$D_{n,j} = (c_1\beta_{n,j} - c_2\alpha_{n,j})^2 + 4c_1c_2\delta_{n,j}^2$$

The four sequences of growth/decay rates $\{\lambda_{n,j}^{\pm}\}$, $n = 0, 1, 2, ...$, $j = M, L$ corresponding to the four sequences of eigenvalues $\{\mu_{n,j}^{\pm}\}$, $n = 1, 2, ...$, $j = M, L$ are given as

$$\lambda_{n,j}^{\pm} = \frac{\mu_{n,j}^{\pm}}{|U'(a)||U'(b)|} - 1 \tag{34}$$

PROOF. Introduce the Fourier series representations

$$\underline{\Psi}(y) = \sum_{n=-\infty}^{n=\infty} \widetilde{\underline{\Psi}}_n \exp[i2\pi ny]$$

$$\mathbb{W}(y) = \sum_{n=-\infty}^{n=\infty} \widetilde{\mathbb{W}}_n \exp[i2\pi ny] \tag{35}$$

24

for $\underline{\Psi}$ and $\mathbb{W}$. The Fourier coefficients $\underline{\widetilde{\Psi}}_n$ and $\widetilde{\mathbb{W}}_n$ are given as

$$\underline{\widetilde{\Psi}}_n = \int\limits_0^1 \underline{\Psi}(y)\exp[-i2\pi ny]dy, \quad \underline{\widetilde{\Psi}}_n \neq \underline{0}$$

$$\widetilde{\mathbb{W}}_n = \int\limits_0^1 \mathbb{W}(y)\exp[-i2\pi ny]dy$$

By plugging (52) into the eigenvalue problem (25) - (27), we find the eigenvalue problem

$$\widetilde{\mathbb{W}}_n\underline{\widetilde{\Psi}}_n = \mu\underline{\widetilde{\Psi}}_n, \quad \underline{\widetilde{\Psi}}_n \neq \underline{0} \tag{36}$$

for all $n = ... -2, -1, 0, 1, 2, ...$, where

$$\widetilde{\mathbb{W}}_n = \begin{bmatrix} c_1\widetilde{\omega}_n(0) & c_2\widetilde{\omega}_n(b-a) & c_2\widetilde{\omega}_n(b+a) & c_1\widetilde{\omega}_n(2b) \\ & & & \\ c_1\widetilde{\omega}_n(b-a) & c_2\widetilde{\omega}_n(0) & c_2\widetilde{\omega}_n(2a) & c_1\widetilde{\omega}_n(b+a) \\ & & & \\ c_1\widetilde{\omega}_n(b+a) & c_2\widetilde{\omega}_n(2a) & c_2\widetilde{\omega}_n(0) & c_1\widetilde{\omega}_n(b-a) \\ & & & \\ c_1\widetilde{\omega}_n(2b) & c_2\widetilde{\omega}_n(b+a) & c_2\widetilde{\omega}_n(b-a) & c_1\widetilde{\omega}_n(0) \end{bmatrix} \tag{37}$$

We notice that $\widetilde{\mathbb{W}}_n = \widetilde{\mathbb{W}}_{-n}$ since by assumption the connectivity kernels $\omega(z, y)$ are even functions of the local variable y. Hence we can assume $n = 0, 1, 2, 3, ...$ without loss of generality. The matrix $\widetilde{\mathbb{W}}_n$ given by (37) can be block diagonalized by means of the matrix $\mathbb{B}$ defined as

$$\mathbb{B} = \begin{bmatrix} 1 & 0 & 0 & -1 \\ 0 & 1 & -1 & 0 \\ 0 & 1 & 1 & 0 \\ 1 & 0 & 0 & 1 \end{bmatrix}. \tag{38}$$

We readily find that

$$\mathbb{B}^{-1}\widetilde{\mathbb{W}}_n\mathbb{B} = \begin{bmatrix} \widetilde{\mathbb{M}}_n & 0 \\ 0 & \widetilde{\mathbb{L}}_n \end{bmatrix} \tag{39}$$

where $\widetilde{\mathbb{M}}_n$ and $\widetilde{\mathbb{L}}_n$ are 2×2 matrices given by (29) and (30), respectively. Standard theory shows that the eigenvalues of the problem (36) are the roots of the quadratic equations

$$\det(\mu\mathbb{I} - \widetilde{\mathbb{M}}_n) = 0, \quad \det(\mu\mathbb{I} - \widetilde{\mathbb{L}}_n) = 0 \tag{40}$$

25

where $\mathbb{I}$ is the unit 2×2 matrix. Simple computation now shows that the eigenvalues of $\widetilde{\mathbb{M}}_n$ ($\widetilde{\mathbb{L}}_n$) are given by the expressions (33) for $j = M$ ($j = L$). By using (27), we find the expressions (34) for the growth/decay rates of the stability problem.

Notice the resemblance of the present Fourier decomposition method with the standard Evans function technique for the homogeneous translational invariant case: The method can be viewed as yielding an Evans function for each Fourier mode given by the LHS of the determinant conditions (40). $\square$

Let us investigate the spectrum of the operator $\mathbb{H}$ in some more detail. For connectivity kernels ω which are piecewise smooth functions of the local variable y like the wizard hat function and the damped oscillating function, we get the bound

$$|\widetilde{\omega}_n(z)| \leq \frac{1}{2\pi n} \int\limits_0^1 |\frac{\partial}{\partial y}\omega(z,y)|dy \tag{41}$$

from which we get the limits

$$\lim_{n\to\infty} \mu^{\pm}_{n,L} = \lim_{n\to\infty} \mu^{\pm}_{n,M} = 0$$

which leads to the property

$$\lim_{n\to\infty} \lambda^{\pm}_{n,L} = \lim_{n\to\infty} \lambda^{\pm}_{n,M} = -1 \tag{42}$$

For $n = 0$, we notice that $\widetilde{\omega}_0(z) = \langle\omega\rangle(z)$. The corresponding eigenvalues are given as

$$\mu^{-}_{0,L} = c_1 c_2 = |U'(a)||U'(b)|$$

$$\mu^{+}_{0,L} =$$

$$\tag{43}$$

$$(\langle\omega\rangle(0) - \langle\omega\rangle(2a))((\langle\omega\rangle(0) - \langle\omega\rangle(2b)) - (\langle\omega\rangle(b+a) - \langle\omega\rangle(b-a))^2$$

$$\mu^{\pm}_{0,M} = \tfrac{1}{2}[c_1(\langle\omega\rangle(0) + \langle\omega\rangle(2b)) + c_2(\langle\omega\rangle(0) + \langle\omega\rangle(2a)) \pm \sqrt{D^{\pm}_0}]$$

26

where

$$D_{0,M} = [c_1(\langle\omega\rangle(0) + \langle\omega\rangle(2b)) - c_2(\langle\omega\rangle(0) + \langle\omega\rangle(2a))]^2$$

$$+4c_1c_2[\langle\omega\rangle(b+a) + \langle\omega\rangle(b-a))]^2$$

According to (34) the growth/decay rates corresponding to (43) are given as

$$\lambda_{0,L}^- = 0$$

$$\lambda_{0,L}^+ = (\tfrac{1}{c_1} + \tfrac{1}{c_2})(\langle\omega\rangle(b-a) - \langle\omega\rangle(b+a)) \qquad (44)$$

$$\lambda_{0,M}^\pm = (c_1c_2)^{-1}\mu_{0,M}^\pm - 1$$

Notice that the expressions for the growth/decay rates $\lambda_{0,j}^\pm, j = L, M$ are identical to those ones appearing in the stability theory for 2 - bumps in the translationally invariant model (1) worked out in Murdock *et al* [9] with $\omega(x)$ replaced with $\langle\omega\rangle(x)$. This is an expected result: When restricting the class of perturbations imposed on the bump state to y - independent perturbations, the eigenvalue problem (25) - (26) simplifies to the eigenvalue problem for the 4×4 matrix

$$\mathbb{H} = \langle\mathbb{W}\rangle = \mathbb{W}_0 =$$

$$\begin{bmatrix} c_1\langle\omega\rangle(0) & c_2\langle\omega\rangle(b-a) & c_2\langle\omega\rangle(b+a) & c_1\langle\omega\rangle(2b) \\ c_1\langle\omega\rangle(b-a) & c_2\langle\omega\rangle(0) & c_2\langle\omega\rangle(2a) & c_1\langle\omega\rangle(b+a) \\ c_1\langle\omega\rangle(b+a) & c_2\langle\omega\rangle(2a) & c_2\langle\omega\rangle(0) & c_1\langle\omega\rangle(b-a) \\ c_1\langle\omega\rangle(2b) & c_2\langle\omega\rangle(b+a) & c_2\langle\omega\rangle(b-a) & c_1\langle\omega\rangle(0) \end{bmatrix} \qquad (45)$$

The eigenvalues of this matrix are given by (43). This restriction corresponds to the stability theory within the framework of the translationally invariant Wilson - Cowan model with the mean value of the connectivity kernel as the integral kernel i.e.

$$\frac{\partial}{\partial t}u(x,t) = -u(x,t) + W(x+b(t);\gamma) - W(x+a(t);\gamma)$$

$$+W(x-a(t);\gamma) - W(x-b(t);\gamma)$$

27

where W is given by (15).

The result $\lambda_{0,L}^{-} \equiv 0$ reflects the translation invariance property of the 2 - bump solution in the global scale.

Next, we study the stability theory in the limit $\gamma \to 0$. We observe that the connectivity kernels ω defined by (11) - (12) constitute a 1 - parameter family of functions, say $\{\omega_\gamma\}_{0 \le \gamma < 1}$, which are continuous in y for each fixed x and which are parameterized by γ:

$$\omega_\gamma(x, y) \equiv \frac{1}{1 + \gamma \cos(y)} \varphi[\frac{x}{1 + \gamma \cos(y)}]$$

Since $|\cos(y)| \le 1$, we find for a fixed x that

$$\omega_\gamma(x, y) \to \varphi[x], \quad \text{uniformly as} \quad \gamma \to 0$$

Hence we are permitted to interchange limit and integration so that

$$\lim_{\gamma \to 0} \widetilde{\omega}_n(x) = \begin{cases} \varphi[x], & n = 0 \\ 0, & n \ne 0 \end{cases} \tag{46}$$

For $n = 0$, we get from (33) that

$$\lambda_{0,L}^{-} \to 0$$

$$\lambda_{0,L}^{+} \to (\tfrac{1}{c_1} + \tfrac{1}{c_2})(\varphi[b - a] - \varphi[b + a]) \tag{47}$$

$$\lambda_{0,M}^{\pm} \to (c_1 c_2)^{-1} \mu_{0,M}^{\pm} - 1$$

uniformly as $\gamma \to 0$. Here

$$\mu_{0,M}^{\pm} = \tfrac{1}{2}[c_1(\varphi[0] + \varphi[2b]) + c_2(\varphi[0] + \varphi[2a]) \pm \sqrt{D_{0,M}}]$$

$$D_{0,M}^{+} = [c_1(\varphi[0] + \varphi[2b]) - c_2(\varphi[0] + \varphi[2a])]^2$$

$$+ 4c_1 c_2[\varphi[b + a] + \varphi[b - a])]^2$$

28

The result (47) is identified with the result obtained by Murdock *et al* [9] for the translationally invariant Wilson - Cowan model (1). From (46) it follows that $\mu_{n,j}^{\pm} \to 0$ uniformly as $\gamma \to 0$ when $n \neq 0$, which means that

$$\lambda_n^{\pm} \to -1 \quad \text{uniformly as} \quad \gamma \to 0, \quad n \neq 0 \tag{48}$$

We get the following theorem on the bound of the growth/decay rates of the stability problem by proceeding in the same way as in Svanstedt *et al* [22]:

Theorem 3. *Let* $\rho_{n,j}^{\pm}, j = M, L; n = 0, 1, 2, ...$ *be the eigenvalues of the normal matrices* $\widetilde{\mathbb{M}}_n^T \widetilde{\mathbb{M}}_n$ *and* $\widetilde{\mathbb{L}}_n^T \widetilde{\mathbb{L}}_n$ *where* $\widetilde{\mathbb{M}}_n$ *and* $\widetilde{\mathbb{L}}_n$ *are given by (29) and (30), respectively. Then the operator norm* $\|\mathbb{H}\|$ *of the operator* $\mathbb{H}$ *is given by*

$$\|\mathbb{H}\| = \sqrt{\max_n(\rho_n)} \tag{49}$$

where ρ_n *is given as*

$$\rho_n \equiv \max_j(\rho_{n,j}^{\pm}), \quad n = 0, 1, 2, ..., \quad j = M, L \tag{50}$$

Moreover, the eigenvalues $\mu_{n,j}^{\pm}$ *given by (33) satisfy the bound*

$$-\|\mathbb{H}\| \leq \mu_{n,j}^{\pm} \leq \|\mathbb{H}\|$$

which corresponds to the bound

$$\lambda_{\min} \leqslant \lambda_{n,j}^{\pm} \leqslant \lambda_{\max}$$

$$\tag{51}$$

$$\lambda_{\min} \equiv -\frac{\sqrt{\max_n(\rho_n)}}{|U'(a)||U'(b)|} - 1, \quad \lambda_{\max} \equiv \frac{\sqrt{\max_n(\rho_n)}}{|U'(a)||U'(b)|} - 1$$

for the growth/decay rates $\lambda_{n,j}^{\pm}$ *of the instability/stability of the 2 - bump solutions.*

PROOF. For any $\underline{\Phi} \in (L^2[0,1])^4$ we first get

$$\| \mathbb{H}\underline{\Phi} \|^2 = \langle \mathbb{H}\underline{\Phi}, \mathbb{H}\underline{\Phi} \rangle = \int_0^1 dy (\int_0^1 dy' \mathbb{W}(y - y')\underline{\Phi}(y')) \cdot (\int_0^1 dy'' \mathbb{W}(y - y'')\underline{\Phi}(y''))$$

29

We then make use of the Fourier - series representations

$$\underline{\Phi}(y) = \sum_{n=-\infty}^{n=\infty} \widetilde{\underline{\Phi}}_n \exp[i2\pi n y]$$

$$\mathbb{W}(y) = \sum_{n=-\infty}^{n=\infty} \widetilde{\mathbb{W}}_n \exp[i2\pi n y]]$$

(52)

and find that

$$\| \mathbb{H}\underline{\Phi} \|^2 =$$

$$\int_0^1 dy[\int_0^1 dy' \sum_{n=-\infty}^{n=\infty} \widetilde{\mathbb{W}}_n \exp[i2\pi n(y-y')] \sum_{m=-\infty}^{m=\infty} \widetilde{\underline{\Phi}}_m \exp[i2\pi m y']]$$

$$\cdot [\int_0^1 dy'' \sum_{k=-\infty}^{k=\infty} \widetilde{\mathbb{W}}_k \exp[i2\pi k(y-y'')] \sum_{l=-\infty}^{l=\infty} \widetilde{\underline{\Phi}}_l \exp[i2\pi l y'']]$$

$$= \sum_{n=-\infty}^{n=\infty} \sum_{m=-\infty}^{m=\infty} \sum_{k=-\infty}^{k=\infty} \sum_{l=-\infty}^{l=\infty} [\widetilde{\mathbb{W}}_n \widetilde{\underline{\Phi}}_m]$$

$$\cdot [\widetilde{\mathbb{W}}_k \widetilde{\underline{\Phi}}_l] \int_0^1 dy' \exp[i2\pi(m-n)y'] \int_0^1 dy'' \exp[i2\pi(l-k)y''] \int_0^1 dy \exp[i2\pi(n+l)y]$$

$$= \sum_{n=-\infty}^{\infty} [\widetilde{\mathbb{W}}_n \widetilde{\underline{\Phi}}_n] \cdot [\widetilde{\mathbb{W}}_n \widetilde{\underline{\Phi}}_{-n}] = \sum_{n=-\infty}^{\infty} [\widetilde{\mathbb{W}}_n \widetilde{\underline{\Phi}}_n]^T [\widetilde{\mathbb{W}}_n \widetilde{\underline{\Phi}}_{-n}] = \sum_{n=-\infty}^{\infty} \widetilde{\underline{\Phi}}_n^T \widetilde{\mathbb{W}}_n^T \widetilde{\mathbb{W}}_n \widetilde{\underline{\Phi}}_{-n}$$

Since by assumption the components of $\mathbb{W}$ are real and even functions of y and the components of $\underline{M}$ are real, the matrix $\widetilde{\mathbb{W}}_n$ has real entries and $\widetilde{\underline{M}}_{-n} = \widetilde{\underline{M}}_n^*$. We notice that the matrix $\widetilde{\mathbb{K}}_n \equiv \widetilde{\mathbb{W}}_n^T \widetilde{\mathbb{W}}_n$ is a real valued and symmetric matrix and that it can be block diagonalized by means of the matrix (38) i.e.

$$\mathbb{B}^{-1}\widetilde{\mathbb{K}}_n\mathbb{B} = \begin{bmatrix} \widetilde{\mathbb{M}}_n^T\widetilde{\mathbb{M}}_n & 0 \\ 0 & \widetilde{\mathbb{L}}_n^T\widetilde{\mathbb{L}}_n \end{bmatrix}$$

(53)

where $\widetilde{\mathbb{M}}_n$ and $\widetilde{\mathbb{L}}_n$ are given by (29) and (30), respectively. We find that

$$\widetilde{\mathbb{M}}_n^T\widetilde{\mathbb{M}}_n = \begin{bmatrix} c_1^2((\widetilde{\beta}_n^+)^2 + (\widetilde{\delta}_n^+)^2) & c_1 c_2 \widetilde{\delta}_n^+(\widetilde{\alpha}_n^+ + \widetilde{\beta}_n^+) \\ c_1 c_2 \widetilde{\delta}_n^+(\widetilde{\alpha}_n^+ + \widetilde{\beta}_n^+) & c_2^2((\widetilde{\alpha}_n^+)^2 + (\widetilde{\delta}_n^+)^2) \end{bmatrix}$$

(54)

30

and

$$\widetilde{\mathbb{L}}_n^T \widetilde{\mathbb{L}}_n = \begin{bmatrix} c_2^2((\widetilde{\alpha}_n^-)^2 + (\widetilde{\delta}_n^-)^2) & c_1 c_2 \widetilde{\delta}_n^-(\widetilde{\alpha}_n^- + \widetilde{\beta}_n^-) \\ c_1 c_2 \widetilde{\delta}_n^-(\widetilde{\alpha}_n^- + \widetilde{\beta}_n^-) & c_1^2((\widetilde{\beta}_n^+)^2 + (\widetilde{\delta}_n^+)^2) \end{bmatrix} \tag{55}$$

The eigenvalues $\rho_{n,j}^\pm$, $n = 0, 1, 2, ...$, $j = M, L$ of $\widetilde{\mathbb{K}}_n$ are the roots in the characteristic equations

$$det(\rho\mathbb{I} - \widetilde{\mathbb{M}}_n^T \widetilde{\mathbb{M}}_n) = 0, \quad det(\rho\mathbb{I} - \widetilde{\mathbb{L}}_n^T \widetilde{\mathbb{L}}_n) = 0$$

We readily find that

$$\rho_{n,M}^\pm = \tfrac{1}{2}[tr(\widetilde{\mathbb{M}}_n^T \widetilde{\mathbb{M}}_n) \pm \sqrt{(tr(\widetilde{\mathbb{M}}_n^T \widetilde{\mathbb{M}}_n))^2 - 4det(\widetilde{\mathbb{M}}_n^T \widetilde{\mathbb{M}}_n)}]$$

$$\tag{56}$$

$$\rho_{n,L}^\pm = \tfrac{1}{2}[tr(\widetilde{\mathbb{L}}_n^T \widetilde{\mathbb{L}}_n) \pm \sqrt{(tr(\widetilde{\mathbb{L}}_n^T \widetilde{\mathbb{L}}_n))^2 - 4det(\widetilde{\mathbb{L}}_n^T \widetilde{\mathbb{L}}_n)}]$$

Here

$$tr(\widetilde{\mathbb{M}}_n^T \widetilde{\mathbb{M}}_n) = c_1^2[\beta_{n,M}^2 + \delta_{n,M}^2] + c_2^2[\alpha_{n,M}^2 + \delta_{n,M}^2]$$

$$det(\widetilde{\mathbb{M}}_n^T \widetilde{\mathbb{M}}_n) = c_1^2 c_2^2[\alpha_{n,M}\beta_{n,M} - \delta_{n,M}^2]^2$$

$$tr(\widetilde{\mathbb{L}}_n^T \widetilde{\mathbb{L}}_n) = c_1^2[\beta_{n,L}^2 + \delta_{n,L}^2] + c_2^2[\alpha_{n,L}^2 + \delta_{n,L}^2]$$

$$det(\widetilde{\mathbb{L}}_n^T \widetilde{\mathbb{L}}_n) = c_1^2 c_2^2[\alpha_{n,L}\beta_{n,L} - \delta_{n,L}^2]^2$$

Simple computation reveals that the eigenvalues $\rho_{n,j}^\pm$, $n = 0, 1, 2, ...$, $j = M, L$ given by (56) are positive, consistent with the fact that the matrices $\widetilde{\mathbb{M}}_n^T \widetilde{\mathbb{M}}_n$ and $\widetilde{\mathbb{L}}_n^T \widetilde{\mathbb{L}}_n$ are normal matrices.

Now, let ρ_n denote the maximal eigenvalue of the matrix $\widetilde{\mathbb{K}}_n$. Since by (56) $\rho_{n,j}^+ \geq \rho_{n,j}^-$, we have

$$\rho_n \equiv \max_j(\rho_{n,j}^\pm) = \max_j(\rho_{n,j}^+), \quad n = 0, 1, 2, ..., \quad j = M, L \tag{57}$$

Hence we obtain the estimate

$$\| \mathbb{H}\underline{\Phi} \|^2 = \sum_{n=-\infty}^{n=\infty} [\rho_{n,M}^+|z_{n,M}^+|^2 + \rho_{n,M}^-|z_{n,M}^-|^2 + \rho_{n,L}^+|z_{n,L}^+|^2 + \rho_{n,L}^+|z_{n,L}^-|^2]$$

$$\leq \sum_{n=-\infty}^{n=\infty} \rho_n|\widetilde{\underline{Z}}_n|^2 = \sum_{n=-\infty}^{n=\infty} \rho_n|\widetilde{\underline{\Phi}}_n|^2 \leq \max_n(\rho_n) \sum_{n=-\infty}^{\infty} |\widetilde{\underline{\Phi}}_n|^2 = \max_n(\rho_n)\|\underline{\Phi}\|^2$$

31

by means of the theory of quadratic forms and Parsevals identity. Here $\widetilde{\underline{\Phi}}_n = \mathbb{P}_n \widetilde{\underline{Z}}_n$ with $\widetilde{\underline{Z}}_n$ given as

$$\widetilde{\underline{Z}}_n = \begin{bmatrix} z_{n,M}^+ \\ z_{n,M}^- \\ z_{n,L}^+ \\ z_{n,L}^- \end{bmatrix}$$

and $\mathbb{P}_n$ being the eigenvector matrix to $\mathbb{K}_n$. We hence conclude that the operator $\mathbb{H}$ is bounded with operator norm $\|\mathbb{H}\|$ given as

$$\|\mathbb{H}\| = \sqrt{\max_n(\rho_n)} \tag{58}$$

We can bound the eigenvalues $\{\mu_{n,j}^{\pm}\}$ of $\mathbb{H}$ by means of the operator norm i.e.

$$\mu_n^2 = \|\mathbb{H}\underline{\Psi}_{n,j}^{\pm}\|^2 \leq \|\mathbb{H}\|^2 = \max_n(\rho_n), \quad \|\underline{\Psi}_{n,j}^{\pm}\| = 1$$

Here the sequence $\{\underline{\Psi}_{n,j}^{\pm}\}$ denotes the normalized eigenfunctions corresponding to the eigenvalues $\{\mu_{n,j}^{\pm}\}$ ($n = 0, 1, 2, ...,, j = M, L$). Then, by restoring to the definition (33) we find the bounding inequality (51) for the growth/decay rates $\lambda_{n,j}^{\pm}$ of the instability/stability of the 2 - bump solutions. $\qquad\square$

We readily show the following properties of the eigenvalues $\rho_{n,j}^{\pm}$, $n = 0, 1, 2, ...,$ $j = M, L$: For $n = 0$, we have

$$tr(\widetilde{\mathbb{M}}_0^T \widetilde{\mathbb{M}}_0) = c_1^2[\langle\beta_M\rangle^2 + \langle\delta_M\rangle^2] + c_2^2[\langle\alpha_M\rangle^2 + \langle\delta_M\rangle^2]$$

$$det(\widetilde{\mathbb{M}}_0^T \widetilde{\mathbb{M}}_0) = c_1^2 c_2^2[\langle\alpha_M\rangle\langle\beta_M\rangle - \langle\delta_M\rangle^2]^2$$

$$tr(\widetilde{\mathbb{L}}_0^T \widetilde{\mathbb{L}}_0) = c_1^2[\langle\beta_L\rangle^2 + \langle\delta_L\rangle^2] + c_2^2[\langle\alpha_L\rangle^2 + \langle\delta_L\rangle^2]$$

$$det(\widetilde{\mathbb{L}}_0^T \widetilde{\mathbb{L}}_0) = c_1^2 c_2^2[\langle\alpha_L\rangle\langle\beta_L\rangle - \langle\delta_L\rangle^2]^2$$

where the mean values $\langle\alpha_j\rangle$, $\langle\beta_j\rangle$ and $\langle\delta_j\rangle$, $j = L, M$ are defined as

$$\langle\alpha_L\rangle = \langle\omega\rangle(0) - \langle\omega\rangle(2a), \quad \langle\alpha_M\rangle = \langle\omega\rangle(0) + \langle\omega\rangle(2a)$$

$$\langle\beta_L\rangle = \langle\omega\rangle(0) - \langle\omega\rangle(2b), \quad \langle\beta_M\rangle = \langle\omega\rangle(0) + \langle\omega\rangle(2b)$$

$$\langle\delta_L\rangle = \langle\omega\rangle(b-a) - \langle\omega\rangle(b+a), \quad \langle\delta_M\rangle = \langle\omega\rangle(b-a) + \langle\omega\rangle(b+a)$$

Moreover, for piecewise smooth connectivity kernels like the wizard hat function and the damped oscillating function, we find by appealing to (41) that

$$\lim_{n\to\infty} \rho_{n,j}^{\pm} = 0$$

from which it follows that

$$\lim_{n\to\infty} \left[\frac{\sqrt{\rho_{n,j}^{\pm}}}{c_1 c_2} - 1 \right] = -1$$

For $\gamma \to 0$ (i.e. the y - independent limit), we have the uniform limits

$$\rho_{n,j}^{\pm} \to 0, \quad \frac{\sqrt{\rho_{n,j}^{\pm}}}{c_1 c_2} - 1 \to -1$$

for $n \neq 0$ and

$$tr(\widetilde{\mathbb{M}}_0^T \widetilde{\mathbb{M}}_0) \to c_1^2 [\beta_M^2 + \delta_M^2] + c_2^2 [\alpha_M^2 + \delta_M^2]$$

$$det(\widetilde{\mathbb{M}}_0^T \widetilde{\mathbb{M}}_0) \to c_1^2 c_2^2 [\alpha_M \beta_M - \delta_M^2]^2$$

$$tr(\widetilde{\mathbb{L}}_0^T \widetilde{\mathbb{L}}_0) \to c_1^2 [\beta_L^2 + \delta_L^2] + c_2^2 [(\alpha_L)^2 + \delta_L^2]$$

$$det(\widetilde{\mathbb{L}}_0^T \widetilde{\mathbb{L}}_0) \to c_1^2 c_2^2 [\alpha_L \beta_L - \delta_L^2]^2$$

where α_j, β_j and δ_j are defined as

$$\alpha_L = \varphi[0] - \varphi[2a], \quad \alpha_M = \varphi[0] + \varphi[2a]$$

$$\beta_L = \varphi[0] - \varphi[2b], \quad \beta_M = \varphi[0] + \varphi[2b]$$

$$\delta_L = \varphi[b - a] - \varphi[b + a], \quad \delta_M = \varphi[b - a] + \varphi[b + a]$$

Interestingly, the operator $\mathbb{H} : (L^2[0,1])^4 \to (L^2[0,1])^4$ is a Hilbert - Schmidt integral operator if the slope parameters $c_1 = |U'(a)|$ and $c_2 = |U'(b)|$ are equal: $c_1 = c_2$. According to the expressions (28) this takes place when the mean value condition $\langle \omega \rangle (2a) = \langle \omega \rangle (2b)$ is fulfilled. In this case

$$\rho_{n,j}^{\pm} = (\mu_{n,j}^{\pm})^2, \quad n = 0, 1, 2, \ldots \quad j = M, L$$

33

where $\mu_{n,j}^{\pm}$, $n = 0, 1, 2, .., j = M, L$ are the eigenvalues of $\mathbb{H}$ given by (33). A notable feature in this special case is that the operator norm $\|\mathbb{H}\|$ belongs to the spectrum of the operator $\mathbb{H}$ i.e.

$$\|\mathbb{H}\| = \sqrt{\max_n(\max_j[(\mu_{n,j}^+)^2])} \tag{59}$$

We are now able to formulate the stability criteria which we will demonstrate in some examples in the next section. These criteria are summarized in the following two general theorems:

Theorem 4. *If $\lambda_{\max}$ given by (58) - (51) is negative, then the 2 - bumps are stable.*

PROOF. Since by (51) we have $\lambda_{n,j}^{\pm} \leq \lambda_{\max}$ for all $n = 0, 1, 2, ..., j = M, L$, we find that $\lambda_{n,j}^{\pm} \leq 0$. $\qquad\square$

Theorem 5. *If at least one of $\lambda_{0,L}^+$ and $\lambda_{0,M}^{\pm}$ given by (44) is strictly positive, then the 2 - bump solutions are unstable.*

We also have the following result for the weakly modulated case i.e. when $0 < \gamma \ll 1$ which follows directly from the continuous dependence of the growth/decay rates on the heterogeneity parameter γ:

Theorem 6. *If $0 \leq \gamma \ll 1$, the stability properties of the 2 - bumps can be inferred from the growth/decay rates $\lambda_{0,L}^+$ and $\lambda_{0,M}^{\pm}$.*

Based on the stability results worked out in this subsection, we now formulate the procedure for assessing the stability of 2 - bump solutions in concrete cases. The procedure can be summarized as follows in the case with different slope parameters i.e. $|U'(a)| \neq |U'(b)|$

- One solves the set of pinning equations (16) - (17) for a θ in the interval of admissible threshold values. The solution $(a_{eq}(\gamma), b_{eq}(\gamma))$ traces out a parameterized curve in the pulse width region $\Sigma = \{(a, b) \; \|b \geqslant a > 0\}$.

- We compute the growth/decay rates $\lambda_{0,L}^+$ and $\lambda_{0,M}^{\pm}$ given by means of the formulas (44) evaluated at the points $(a_{eq}(\gamma), b_{eq}(\gamma))$. If at least one of these rates is strictly positive for a fixed γ, then the 2 - bump solution is unstable for this value of γ. Cf. Theorem 5.

34

- On the contrary, if all $\lambda_{0,L}^+$ and $\lambda_{0,M}^\pm$ are strictly negative for a given value of γ, there are two possibilities: First, if $\lambda_{\max}$ given by (58) - (51) is negative for a given value of γ, then the 2 - bumps state is stable for this value of γ. If it turns out that $\lambda_{\max}$ is positive, then the stability issue can only be resolved by means of the four sequences of growth rates (33) - (34).

Notice that we have the possibility of stabilization/destabilization of 2 - bumps. This may happen for example if $\lambda_{0,L}^+$ and $\lambda_{0,L}^\pm$ are strictly negative while $\lambda_{\max}$ given by (58) - (51) is strictly positive.

On the other hand in the case with equal slope parameters ($|U'(a)| = |U'(b)|$), the operator norm $\|\mathbb{H}\|$ belongs to the spectrum of the operator $\|\mathbb{H}\|$ and we can get a sharp stability criterion: We have stability (instability) if (51) with $\|\mathbb{H}\|$ given by (59) is negative (positive).

3.2. Examples

In this subsection we study numerically the stability of 2 - bump solutions in two concrete cases.

In the first case we assume that the scaling function φ is given as the wizard hat function (11) - (13). As pointed out in Section 2 the generic picture consists of a narrow and broad 2 - bumps state. Here we choose to do the stability assessment of the bumps states illustrated in Fig. 5 and Fig. 7. Fig. 9 shows the graphs of $\lambda_{0,L}^+$ and $\lambda_{0,M}^\pm$ as functions of the heterogeneity parameter γ for the broad 2 - bump solutions, whereas Fig. 10(a) shows the graphs of $\lambda_{0,L}^+$ and $\lambda_{0,M}^\pm$ as functions of the heterogeneity parameter γ for the narrow 2 - bump solutions. In Fig. 10(b) we show that $\lambda_{0,L}^- \neq \lambda_{0,M}^-$ in Fig. 10(a). We observe that $\lambda_{0,L}^+$ and $\lambda_{0,M}^+$ are strictly positive for all γ. We conclude that the 2 - bump solutions are unstable for all γ, which means that the finite heterogeneity does not alter the stability properties as compared with the translationally invariant case. This result is in accordance with the result obtained in Murdock *et al* [9].

In the second case we assume that the connectivity function (11) is expressed in terms of the damped oscillatory function scaling function (14). We first determine one of the 1 - parameter family of solutions to the pinning equations

(16) - (17) for a given θ belonging to the set of admissible threshold values i.e. we find (a, b) as a function of the heterogeneity parameter γ. In this numerical computation we have chosen $K = 1$, $\alpha = 1$, $\beta = 0.25$. The actual 1 - parameter family of solutions corresponds to a stable 2 - bump solution in the translationally invariant case ($\gamma = 0$). It turns out that this family of solutions exists for some γ - interval, say $0 \leq \gamma \leq \gamma_{ex}$, where $\gamma = 0.43$. For $\gamma = \gamma_{ex}$, it turns out that the level curve $G(a, b; \gamma) = 0$ terminates at the level curve $F(a, b; \gamma) = \theta$ while for $\gamma > \gamma_{ex}$, there is no local intersection of these level curves. In Fig. 11 we depict the 1 - parameter family of solutions (a, b) as a parameterized curve in the pulse width coordinate plane, with γ as a parameter, $0 \leq \gamma \leq \gamma_{ex}$. In Fig. 12 we have plotted the sequence of corresponding 2 - bumps for specific choice of the heterogeneity parameter γ, corresponding to selected points on the curve in Fig. 11. In Fig. 13 the graphs of $\lambda_{0,L}^{+}$ and $\lambda_{0,M}^{\pm}$ together with the graphs of the maximum of $\lambda_{n,j}^{\pm}$ ($j = L, M$) for the curve depicted in Fig. 11 are shown for the interval $0 \leq \gamma \leq \gamma_{ex}$ for $n = 1, 2, 3, 4, 5$. We observe that $\lambda_{0,L}^{+}$ and $\lambda_{0,M}^{\pm}$ are strictly negative. Thus, in order to assess the stability of the 2 - bumps state as a function of the heterogeneity parameter, we examine the behavior of the rates $\lambda_{n,j}^{\pm}$, $n = 1, 2, 3, ..., j = M, L$ as a function of γ. As $\lambda_{n,j}^{\pm} < 0$ for large n, it suffices to plot $\lambda_{n,j}^{\pm}$ for low values of n. Based on this investigation, we conjecture that the 2 - bumps are stable for the whole interval $0 < \gamma \leq \gamma_{ex}$). Notice that for the case of a damped oscillating connectivity kernel, it is possible to have more than two 2 - bumps solutions for each admissible threshold value. We do not pursue a detailed study here with respect to existence and stability of these bumps structure as a function of the heterogeneity, however.
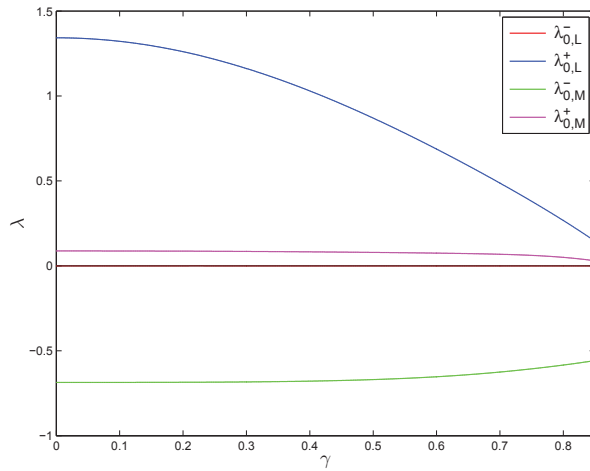
Figure 9: The rates $\lambda_{0,L}^{\pm}$ and $\lambda_{0,M}^{\pm}$ as functions of the heterogeneity parameter γ for broad 2 - bump solutions when $\theta = 0.05$. The scaling function φ is given by the wizard hat function (13) with $\alpha = 2$.
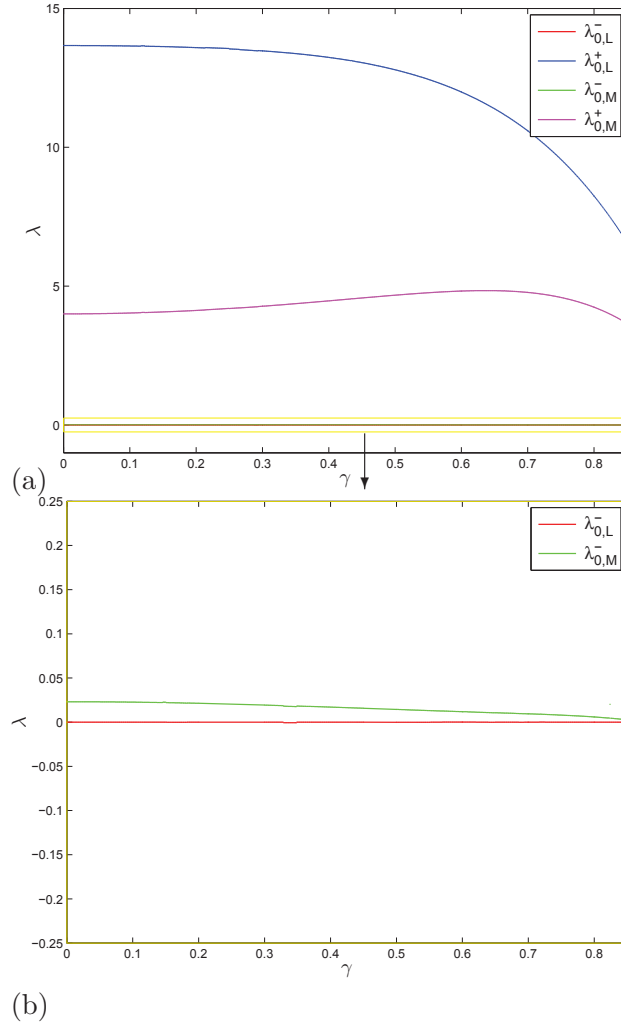
Figure 10: The rates $\lambda^{\pm}_{0,L}$ and $\lambda^{\pm}_{0,M}$ as functions of the heterogeneity parameter γ for the narrow 2 - bump solutions when $\theta = 0.05$. The scaling function φ is given by the wizard hat function (13) with $\alpha = 2$. Fig. 10(b) gives a magnified view of rectangular region marked in Fig. 10(a).
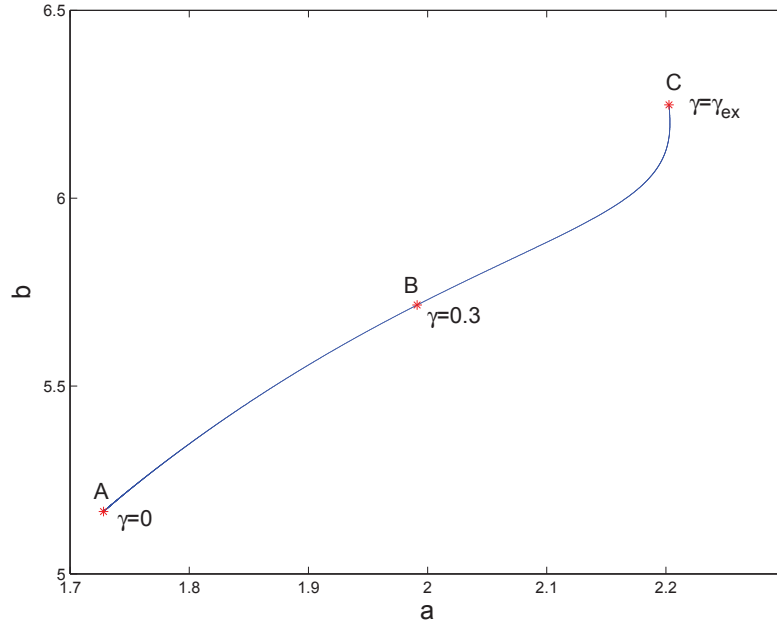
Figure 11: The solution (a, b) of the pinning equations (16) - (17) as a parameterized curve in the pulse width coordinate plane, with γ as a parameter with $0 \leq \gamma \leq \gamma_{ex}$ and a fixed threshold value θ ($\theta = 0.5$). The scaling function φ is given by the damped oscillating function (14) with $K = \alpha = 1$ and $\beta = 0.25$. For $\gamma = \gamma_{ex} = 0.43$ the level curve $G(a, b; \gamma) = 0$ terminates at the level curve $F(a, b; \gamma) = \theta$ while for $\gamma > \gamma_{ex}$, there is no local intersection of these level curves. The points A, B and C correspond to $\gamma = 0$, $\gamma = 0.3$ and $\gamma = \gamma_{ex} = 0.43$, respectively.
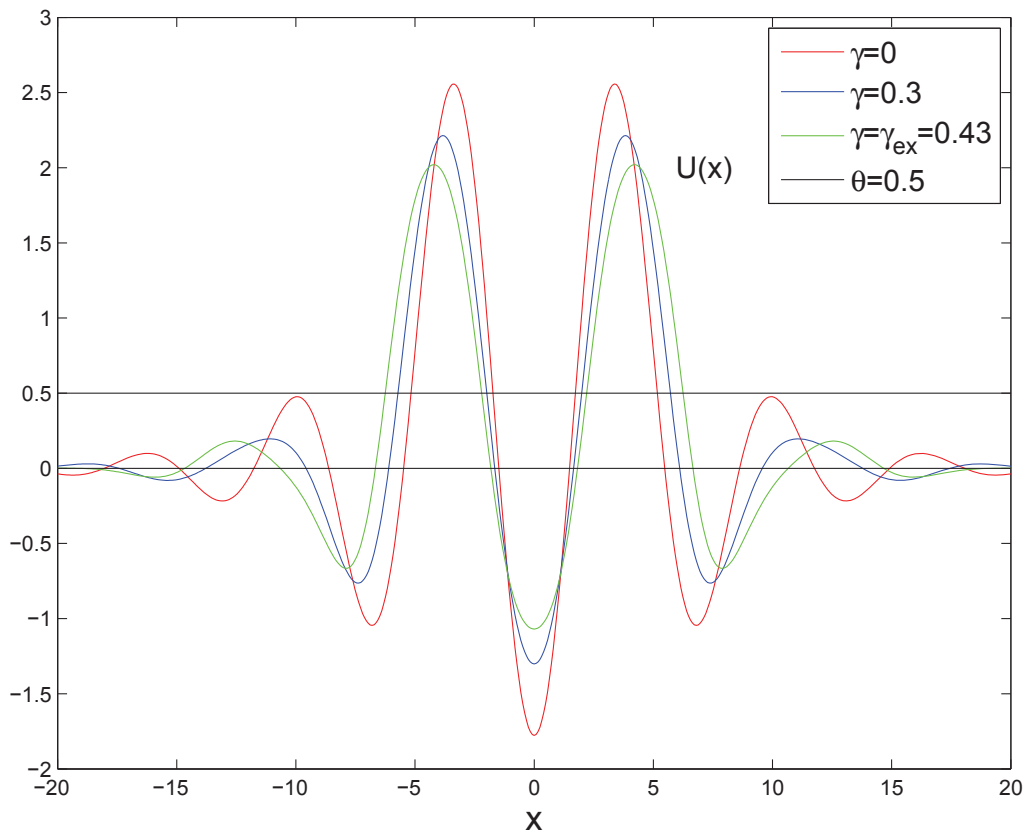
Figure 12: 2 - bump solutions corresponding to the points A,B and C on the curve in Fig. 11.
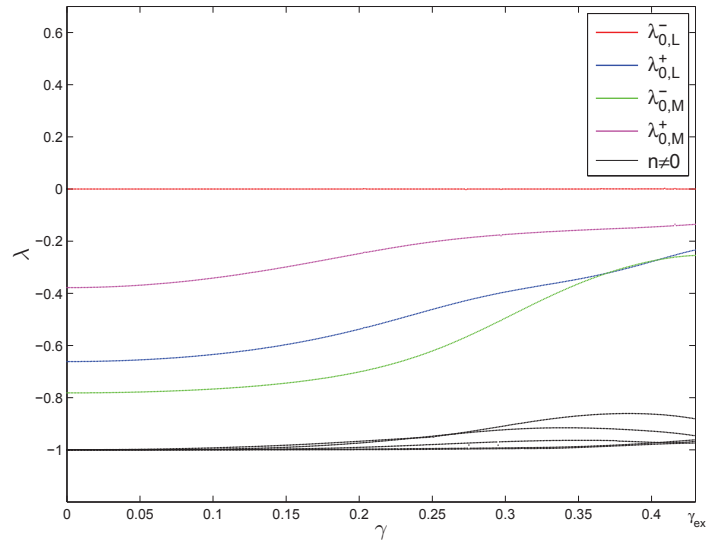
Figure 13: The rates $\lambda_{0,L}^{\pm}$, $\lambda_{0,M}^{\pm}$, and $\lambda_{n,j}^{\pm}$ ($j = L, M$, $n = 1, 2, 3, 4, 5$) as functions of the heterogeneity parameter γ for $0 \leq \gamma \leq \gamma_{ex}$, corresponding to the parameterized curve displayed in Fig. 11. The scaling function φ is given by the damped oscillating function (14) with $K = \alpha = 1$, $\beta = 0.25$.

4. Conclusions and outlook

The present paper is devoted to the study of the existence and stability of 2 - bump solutions of a homogenized Wilson-Cowan model when approximating the firing rate function with a Heaviside function.

It turns out that the existence theory can efficiently be studied by interpreting the pinning condition as a mapping of the pulse width coordinates of the 2 - bumps to the threshold value plane in a way analogous to Blomquist *et al* [26] and Yousaf *et al* [27] for single bumps in a two population model. When assuming the connectivity kernel to be periodically modulated in both the synaptic footprint and the spatial scale with a scaling function given by the wizard hat function, we find regimes of existence of 2 - bump solutions as a function of the threshold value θ and the heterogeneity parameter γ. A notable feature is that for each γ there is an interval of small and moderate values of threshold values $0 < \theta \leq \theta_{cr} < 1$ for existence of 2 - bump solutions, where θ_{cr} depends on γ. For the regime $\theta_{cr} < \theta \leq 1$ we have non - existence of 2 - bumps. We also show that the generic picture consists of one broad and one narrow 2 - bump solution when $0 < \theta < \theta_{cr}$.

We then develop a stability method for 2 - bump solutions. The whole problem boils down to a study of the spectral properties of a Fredholm integral operator. The eigenvalues of this problem which are found by means of the Fourier decompositions method are real and directly related to the growth/decay rates of the perturbations imposed on the bumps state. The only possible element in the essential spectrum is according to standard theory for linear compact operators on Hilbert spaces the accumulation point 0 of these eigenvalues. The essential spectrum thus does not influence the stability assessment of the bumps. We find a bounding inequality for the growth/decay rates of the perturbations, where the upper and lower bounds are expressed in terms of the operator norm of the actual Fredholm integral operator. One easily recovers the four eigenvalues of the actual integral operator obtained by the Evans function approach for the homogeneous, translationally invariant case by considering the subclass of perturbations which are independent of the local scale y. One of these eigenvalues corresponds to the translational invariance property of the bumps solution. We then show that both the narrow and the broad 2 - bump solutions are unstable when the scaling function of the connectivity function is given by means of

a wizard hat function for all admissible values of the heterogeneity parameter, just as in the translationally invariant case [9]. Finally, we provide an example where the connectivity function is expressed in terms of a damped oscillatory scaling function. We identify the regime of existence of 2 - bumps numerically as a function of the heterogeneity parameter. The actual 2 - bump solution is designed to be stable when switching off the heterogeneity. We demonstrate by using the stability method that this 2 - bump solution remains stable when switching on the heterogeneity parameter.

The Fourier decomposition method for stability developed in the present paper can be viewed as yielding an Evans function for each Fourier mode in a way analogous to the homogeneous case. We point that this method has previously been used in the study of the stability of a single bumps in the homogenized Wilson - Cowan model (3) [22], the spectral stability of vortex solutions to the Gross - Pitaevski equation in a two dimensional spatial configuration [25] and the stability of single bump solutions of the homogeneous and translational invariant Wilson - Cowan model in two spatial dimensions [24].

In future works we aim at investigating the existence of 2 - bump solutions within the framework of the homogenized model with a steep and smooth firing rate function by means of nonlinear functional analysis and degree theory. We conjecture that this problem can be tackled by proceeding in a way analogous to Oleynik *et al* [30]. We will also investigate the stability of single bumps on two spatial dimensions within the framework of the homogenized Wilson - Cowan model (3). This study will be complemented with the development of appropriate numerical schemes which can be used to detail the numerical evolution of both stable and unstable bumps within the framework of the homogenized model. Finally, but not least we aim at comparing the results in the present paper with simulation results for original networks with heterogeneous microstructure the model (2). Work on some of these aspects is under progress.

5. Acknowledgements

References

[1] H. R. Wilson and J. D. Cowan, *A mathematical Theory of the Functional Dynamics of Cortical and Thalamic Nervous Tissue*, Kybernetik 13 (1973) 55–80.

[2] S. Amari, *Dynamics of pattern formation in lateral-inhibition type neural fields*, Biological Cybernetics **27** (1977) 77 – 87.

[3] S. Coombes, *Waves, bumps, and patterns in neural field theories*, Biological Cybernetics **93** (2005) 91 – 108.

[4] J. A. Murdock, *Multi-Parameter Oscillatory Connection Functions in Neural Field Models*, Contemporary Mathematics 440 (2007) 177 – 186.

[5] J. B. Levitt, D. A. Lewis, T. Yoshioka and J. S. Lund, *Topography of pyramidal neuron intrinsic connections in macaque prefrontal cortex*, Journal of Comparative Neurology 338 (1993) 360 – 376.

[6] A. J. Elvin, C. R. Laing, R. I. McLachlan and M. G. Roberts, *Exploiting the Hamiltonian structure of a neural field model*, Physica D 239 (2010) 537 – 546.

[7] C. R. Laing, W. C. Troy, B. Gutkin and G. B. Ermentrout, *Multiple bumps in a neuronal network model of working memory*, SIAM J. Appl. Math. **63** (2002) 62 – 97.

[8] C. R. Laing and W. C. Troy, *Two-bump solutions of Amari- type models of neuronal pattern formation*, Physica D 178 (2003) 190 – 218.

[9] J. A. Murdock, F. Botelho and J. E. Jamison, *Persistence of spatial patterns produced by neural field equations*, Physica D 215 (2006) 106 – 116.

[10] J. Xin, *An Introduction to Fronts in Random Media*, SIAM Review, 42, 161 (2000).

[11] J. Xin, *An Introduction to Fronts in Random Media*, Surveys and Tutorials in the Applied Mathematical Sciences, Springer Verlag (2009).

[12] P. C. Bressloff, *Traveling fronts and wave propagation failure in an inhomogeneous neural network*, Physica D 155 (2001) 83 – 100.

[13] P. C. Bressloff, *Spatially periodic modulation of cortical patterns by long-range horizontal connections.* Physica D 185 (2003) 131 – 157.

[14] P. C. Bressloff, S. E. Folias, A. Pratt and Y-X Li, *Oscillatory waves in inhomogeneous neural media* Phys. Rev. Lett. 91:178101 (2003).

[15] X. Huang, W. C. Troy, Q. Yang, H. Ma, C. R. Laing, S. J. Schiff and J.-Y. Wu, *Spiral waves in disinhibited mammalian neocortex* J. Neurosci. 24 (44) (2004) 9897 – 9902.

[16] Z. P. Kilpatrick, S. E. Folias and P. C. Bressloff, *Traveling pulses and wave propagation failure in an inhomogeneous neural network*, SIAM J. Appl. Dyn. Syst. 7 (2008) 161 – 185.

[17] S. Coombes and C. R. Laing, *Pulsating fronts in periodically modulated neural field models*, Phys. Rev. E. 83 (2010), 011912.

[18] L.- E. Persson. L. Persson, N. Svanstedt, and J. Wyller, *The Homogenization Method. An introduction.* Studentlitteratur. (1993).

[19] G. Nguetseng, *A general convergence result of a functional related to the theory of homogenization*, SIAM J. Math. Anal. 20 (1989) 608 – 623.

[20] D. Lukkassen, G. Nguetseng and P. Wall, *Two-scale convergence*, Int. J. Pure Appl. Math. 2 (2002) 35 – 86.

[21] N. Svanstedt and J. L. Woukeng, *Homogenization of a Wilson - Cowan model for neural fields in a bounded domain.* Nonlinear Analysis Real World Applications 14 (2013) 1705 – 1715.

[22] N. Svanstedt, J. Wyller and E. Malyutina, *A one-population Wilson Cowan model with periodic microstructure*, Submitted to Nonlinearity, (2013).

[23] S. Coombes, C. Laing, H. Schmidt, N. Svanstedt and J. Wyller, *Waves in random neural media*, Discrete and Continuous Dynamical Systems – Series A 32 (2012) 2951 – 2970.

[24] M. R. Owen, C. R. Laing and S. Coombes, *Bumps and rings in a two-dimensional neural field: splitting and rotational instabilities*, New Journal of Physics, 9 (2007), 378.

[25] R. Kollár and R. L. Pego, *Spectral Stability of Vortices in Two-Dimensional BoseEinstein Condensates via the Evans Function and Krein Signature*, Applied Mathematics Research eXpress, 2012, No. 1 (2012) pp. 1 - 46.

[26] P. Blomquist, J. Wyller and G. T. Einevoll, *Localized activity patterns in two-population neural networks*, Physica D 206 (2005) 180 – 212.

[27] M. Yousaf, J. Wyller, T. Tetzlaff and G. T. Einevoll, *Effect of localized input on bump solutions in a two-population neural-field model*, Nonlinear Analysis: Real World Applications 14 (2013) 997 – 1025.

[28] D. Porter and D. S. G. Stirling, *Integral Equations*, Cambridge Texts in Applied Mathematics, 1990.

[29] A. N. Kolomogorov and S. V. Fomin, *Elements of the Theory of Functions and Functional Analysis*, Vol. 1, Courier Dover Publications, 1999.

[30] A. Oleynik, A. Ponosov and J. Wyller, *On the properties of nonlinear nonlocal operators arising in neural field models*, J. Math. Anal. Appl. 398 (2013) 335 – 351.